MAGNETIC VARIABLES CONTROL

Applications of variable-speed electric drive systems are constantly diversifying and growing in numbers. Such a trend is primarily caused by ever-increasing levels of factory automation during the past few decades. It is difficult today to find a single manufacturing process that does not involve at least one variable-speed electric drive. Electric drives power elevators, overhead cranes, machine tools, robots, conveyer belts, steel production lines, paper mills, pumps, compressors, and so on. The other important and expanding area of application is transportation systems. Electric machines drive trains, electric vehicles, and electric forklifts and are indispensable in various motion control systems of airplanes, ships, satellites, and space craft. Last but not least, the application area correlated with domestic appliances has experienced considerable development during the last two decades as well. Electric machines power washing machines and tumble dryers, hand tools, lawn movers, and hair dryers, to name a few. What all these very different applications have in common is that variable-speed operation is required.

Different applications of variable-speed electric drives impose differing requirements on accuracy of the speed control. In a number of cases the rotating speed of a drive has to be close to but not necessarily equal to the reference speed. Typical examples are fans, pumps, and compressors, for which it is frequently sufficient to have only an approximate control of speed as even a small change in speed causes considerable variation in the output power. Electric drives that are utilized in these applications today are usually called general-purpose *ac* drives. Their characteristics are lack of closed-loop speed control, low cost, low maintenance requirements, and high reliability. The second type of variable-speed electric drive is the one that is used when rough speed control does not suffice. Closed-loop speed control is then necessary so that the shaft of the machine is equipped with a speed-measuring device. Speed control is accurate in the steady state only and no attempt is made to control the transition from one reference speed to the other. The transient response of such a drive is therefore poor, but the speed holding is good in the steady state. In contrast to this, the third type of a variable-speed drive, usually called high-performance drive, is capable of providing both accurate steady-state speed control and a controlled transition from one reference speed to the other. Applications that necessitate use of a high-performance drive include robotics, machine tools, elevators, rolling mills, paper mills, spindles, mine winders, electric traction, and electric vehicles. As the transition from one speed to another has to be controllable, it is necessary to control not only speed but transient torque as well. (If a drive is used for positioning, rotor position control is also required.) Such high-performance applications typically require steady-state speed control accuracy better than 0.5%, a wide range of speed control (typically at least 20:1), and very fast and accurate transient response (1).

A separately excited *dc* motor was until recently the only available electric machine that could be used in a high-performance drive. A dc motor is, by virtue of its construction, ideally suited to meeting control specifications for high performance. However, dc motor construction is at the same time the reason why dc drives are today replaced with ac drives wherever possible. A separately excited dc motor has two windings: One is on the stator and the other one is on the rotor. Stator winding is supplied with dc current and provides excitation flux. The rotor (armature) winding is supplied with dc current as well, through the commutator assembly that encompasses stationary brushes that move along the commutator surface as the rotor rotates. The commutator with brushes is the major weakness of a dc motor. It requires maintenance, and the brushes have to be replaced on a regular basis. Because the brushes slip along the commutator during rotation, the maximum current that can be supplied during transient operation is limited, as is the allowable rate of change of current. The commutator limits the maximum operating speed as well. The cost, size, and weight of a dc machine are all higher than for an ac machine of the induction motor type with an equivalent power rating. The inertia of a dc machine is higher than the inertia of an ac machine. This means that under equal developed torque conditions, a dc motor will take longer to reach the desired speed than an ac motor. The efficiency and overall power factor of an ac drive are, in general, better than for the equivalent dc drive (1). These are the reasons behind the general trend of replacing dc motors with ac motors. Nevertheless, the idea behind the concept of a high-performance drive is most easily explained by taking a separately excited dc motor as an example.

High performance requires a controlled transition from one steady-state operating speed to another. Because the motion of the rotor takes place due to the developed electromagnetic torque of the machine, the motor torque has to be controlled during the transient. The electromagnetic torque of a separately excited dc motor is determined with the product of the armature current and the excitation flux. The existence of the commutator with brushes, which are positioned in an axis perpendicular to the axis along which excitation flux acts, makes it possible to control excitation flux and developed torque independently by means of two dc currents. Excitation flux is determined solely by the value of the excitation current and does not change if armature current varies. Suppose that the machine is excited with constant excitation current, so that excitation flux is constant as well. Developed electromagnetic torque is then controllable solely by armature current. The desired torque value in both steady-state and transient operation is achieved by supplying the armature winding with an appropriate current value. Hence the existence of the commutator assembly inherently enables independent flux and torque control. It is usually said that flux and torque control are decoupled as flux is controlled by one (excitation winding) current while torque is, in constant flux operation, controlled by another (armature winding) current.

The important conclusion that results from the discussion of torque production in a dc machine is that decoupled flux and torque control requires control of armature current. This means that a current-controlled dc source must feed the machine's armature winding. In other words, the output voltage of the dc source is controlled in a closed-loop

manner in such a way that the required armature current is produced. Current-controlled sources that are used to supply a dc machine are power electronic converters of an ac/dc type that come in various configurations.

The preceding discussion can be summarized in five statements: (1) High-performance operation requires that electromagnetic torque of a motor is controllable in real time; (2) instantaneous torque of a separately excited dc motor is directly controllable by armature current as flux and torque control are inherently decoupled; (3) independent flux and torque control are possible in a dc machine due to its specific construction, which involves a commutator with brushes whose position is fixed in space; (4) instantaneous flux and torque control require that the machine windings are fed from current-controlled dc sources; and (5) current and speed sensing is necessary in order to obtain feedback signals for real-time control.

Substitution of dc drives with ac drives in high-performance applications has become possible only recently. From the control point of view, it is necessary to convert an ac machine into its equivalent dc counterpart so that independent control of two currents yields decoupled flux and torque control. What the commutator with brushes does in a dc machine physically (statements 2 and 3) has to be done in an ac machine mathematically. This is unfortunately far from being a trivial task. The most frequently utilized types of ac machines are of brushless construction, so the physical structure of the machine is not any help in establishing means for independent flux and torque control. Fundamental principles that enable mathematical conversion of an ac three-phase machine into an equivalent dc machine were established in the early 1970s for both induction and synchronous machines (2) and are known as vector control or field-oriented control (1–5). What remains common for both dc and ac high-performance drives is that the supply sources are current controlled (statement 4), current feedback and speed feedback are required (statement 5), and torque is controlled in real time (statement 1). Stator winding of three-phase ac machines is supplied with ac currents, which are characterized by amplitude, frequency, and phase rather than just by amplitude, as in dc case. Thus an ac machine has to be fed from a source of variable output voltage, variable-output frequency type. Power electronic converters of dc/ac type (inverters) are the most frequent source of power in high-performance ac drives. Application of vector-controlled ac machines in high-performance drives became a reality in the early 1980s and has been enabled by developments in the areas of power electronics and microprocessors. Control systems that enable realization of decoupled flux and torque control in ac motor drives are complex and involve a coordinate transformation that has to be executed in real time. Application of microprocessors or digital signal processors is therefore mandatory.

The frequency of the stator winding supply uniquely determines the speed of rotation of a synchronous machine. Permanent magnets or dc excitation current in the rotor winding provide excitation flux. The rotor carries with it the excitation flux as it rotates, and the instantaneous spatial position of the rotor flux is always fixed to the rotor. Hence, if rotor position is measured, the position of the excitation flux is known. Such a situation leads to relatively simple vector control algorithms for both permanent magnet and wound rotor synchronous motors (1, 3, 4). The situation is more involved in synchronous reluctance machines. The rotor is of salient pole structure but without either magnets or excitation winding, so that excitation flux stems from the ac supply of the three-phase stator winding. By far the most complex situation results in induction machines where not only the excitation flux stems from the stator winding supply but the rotor rotates asynchronously with the rotating field. This means that even if the rotor position is measured, the position of the rotating field in the machine remains unknown. Vector control of induction machines is thus the most complicated case (1–5).

Vector control of ac machines has reached a mature stage and is today widely applied when high performance is required. A squirrel-cage induction machine is the most frequently used type of electric machines and is found in applications that cover the entire power range. The main advantages of an induction motor over the other types of ac motors are low cost and very rugged construction that requires virtually no maintenance. Application of synchronous motors takes place either in relatively low-power regions (permanent magnet machines) or in very high-power regions (wound rotor synchronous machines). Although permanent magnet machines are brushless as well, their cost is at present considerably higher than the cost of an induction motor of the same power rating. Wound rotor synchronous machines are of the brushed type and are applied as motors in very high-power regions only, where their higher cost is offset by some advantages over the induction motors. It follows from this consideration that induction machines are used whenever possible, and it is for this reason that only vector control of induction machines is dealt with in this article.

Vector control of ac machines enables decoupled torque and flux control in much the same way as it is achieved in dc machines. To explain vector control principles, it is necessary to perform at first transformation of the model of an ac machine from the original phase domain into a fictitious, so-called arbitrary reference frame domain.

MATHEMATICAL MODELING OF AN INDUCTION MACHINE

Vector control provides instantaneous control of the machine's flux and torque, which is to be realized via instantaneous current control. Thus the time domain mathematical model, in terms of original phase variables, has to be utilized as a starting point. Unfortunately, principles of vector control cannot be explained and understood from this time domain model. Instead, this model has to be mathematically transformed into a new model, which describes a fictitious induction machine equivalent to the original one, by a suitably chosen mathematical transformation.

The procedure of mathematical modeling of an induction machine is subject to a number of assumptions (4, 6, 7). Those that are relevant for subsequent considerations are that winding resistances and leakage inductances are constant parameters, iron losses and higher spatial har-

monics of magnetomotive force (*m.m.f.*) are neglected, and it is assumed that the magnetizing curve of the machine is linear (flux saturation is neglected). By performing mathematical transformation of the model given in terms of existing phase quantities, the physical induction machine is substituted with an equivalent induction machine that does not exist in reality. Both stator and rotor three-phase windings are transformed, using different mathematical transformations for stator and rotor. The resulting mathematical model may be given in terms of either real (6) or complex (7) variables. The main feature of the transformed model is that it describes a fictitious machine whose equivalent stator and rotor windings all rotate at the same, in general arbitrary, angular speed. Relative motion between stator and rotor phase windings is substituted with fictitious electro-motive forces. The transformation is therefore referred to as transformation to the common arbitrary reference frame. The following two subsections review the real, so-called d-q-axis model and the complex, so-called space vector model of a three-phase induction machine.

Real d-q-Axis Model

Let the phases of the original three-phase windings on stator and rotor be denoted with indices a, b, c and A, B, C, respectively. Symbols v, i, and ψ stand for instantaneous voltage, current, and flux linkage of any of the windings. Stator and rotor three-phase windings are to be transformed into a common reference frame, which rotates at an arbitrary angular speed ω_a, so that resulting new stator and rotor windings (ds, qs, and dr, qr) will all rotate with the same arbitrary angular speed. Hence the transformation enables substitution of a six-winding induction machine with an equivalent four-winding machine.

The magnetic axis of the stator phase winding a is taken as a stationary axis with respect to which all the angular positions are measured. As the rotor rotates at an electrical angular speed ω, instantaneous position of the rotor winding A magnetic axis with respect to the stator phase a magnetic axis is determined with $\theta = \int \omega dt$. All the windings are transformed to the arbitrary reference frame rotating at speed ω_a, so that instantaneous position of d-axis with respect to the stationary phase a axis is determined with $\theta_s = \int \omega_a dt$. The angle between d-axis and the rotor A axis is hence $\theta_r = \theta_s - \theta$. The axes d and q are mutually perpendicular. Let f denote either voltage, current, or flux linkage of any of the windings of stator and rotor. The transformation of original to equivalent d-q-axis windings is governed with transformation angles θ_s and θ_r for stator and rotor quantities, respectively. In particular,

$$\begin{aligned} f_{ds} &= \frac{2}{3}\left[f_a \cos\theta_s + f_b \cos(\theta_s - 2\pi/3) + f_c \cos(\theta_s - 4\pi/3)\right] \\ f_{qs} &= -\frac{2}{3}\left[f_a \sin\theta_s + f_b \sin(\theta_s - 2\pi/3) + f_c \sin(\theta_s - 4\pi/3)\right] \end{aligned} \tag{1}$$

$$\begin{aligned} f_{dr} &= \frac{2}{3}\left[f_A \cos\theta_r + f_B \cos(\theta_r - 2\pi/3) + f_C \cos(\theta_r - 4\pi/3)\right] \\ f_{qr} &= -\frac{2}{3}\left[f_A \sin\theta_r + f_B \sin(\theta_r - 2\pi/3) + f_C \sin(\theta_r - 4\pi/3)\right] \end{aligned} \tag{2}$$

where indices s and r stand for stator and rotor, respectively. Equations (1) and (2) define transformation from the original phase domain into the common d-q-axis reference frame as a single-step transformation. The transformation may be looked at as being composed of two transformations. The first one replaces original three-phase windings with equivalent two-phase windings that still rotate with the speed of rotation of the original windings, while the second transformation replaces two-phase machine with d-q-axis windings that all rotate at the same speed.

The factor ⅔ in Eqs. (1) and (2) is correlated with powers in the original and the equivalent induction machine. While the actual machine is three phase, the equivalent one is two-phase. Factor ⅔ preserves the equality of power per phase in the original and the equivalent machine. As the rotor winding is short-circuited (either squirrel-cage machine or slip-ring machine with short-circuited rotor winding is assumed), instantaneous power in terms of transformed quantities equals

$$P_e = (3/2)(v_{ds} i_{ds} + v_{qs} i_{qs}) \tag{3}$$

The mathematical model of a three-phase induction machine is, upon completion of the transformation, obtained in the following form:

$$\begin{aligned} v_{ds} &= R_s i_{ds} + \frac{d\psi_{ds}}{dt} - \omega_a \psi_{qs} \\ v_{qs} &= R_s i_{qs} + \frac{d\psi_{qs}}{dt} + \omega_a \psi_{ds} \end{aligned} \tag{4}$$

$$\begin{aligned} v_{dr} = 0 &= R_r i_{dr} + \frac{d\psi_{dr}}{dt} - (\omega_a - \omega)\psi_{qr} \\ v_{qr} = 0 &= R_r i_{qr} + \frac{d\psi_{qr}}{dt} + (\omega_a - \omega)\psi_{dr} \end{aligned} \tag{5}$$

where d-q-axis flux linkages are given by

$$\begin{aligned} \psi_{ds} &= L_s i_{ds} + L_m i_{dr} = L_{\sigma s} i_{ds} + L_m (i_{ds} + i_{dr}) \\ \psi_{qs} &= L_s i_{qs} + L_m i_{qr} = L_{\sigma s} i_{qs} + L_m (i_{qs} + i_{qr}) \end{aligned} \tag{6}$$

$$\begin{aligned} \psi_{dr} &= L_r i_{dr} + L_m i_{ds} = L_{\sigma r} i_{dr} + L_m (i_{ds} + i_{dr}) \\ \psi_{qr} &= L_r i_{qr} + L_m i_{qs} = L_{\sigma r} i_{qr} + L_m (i_{qs} + i_{qr}) \end{aligned} \tag{7}$$

and magnetizing flux, magnetizing current, and magnetizing inductance (all denoted with an index m) are defined as

$$\begin{aligned} i_{dm} &= i_{ds} + i_{dr} & i_{qm} &= i_{qs} + i_{qr} \\ \psi_{dm} &= L_m i_{dm} & \psi_{qm} &= L_m i_{qm} \\ i_m &= \sqrt{i_{dm}^2 + i_{qm}^2} & \psi_m &= \sqrt{\psi_{dm}^2 + \psi_{qm}^2} \\ L_m &= \psi_m / i_m \end{aligned} \tag{8}$$

The magnetizing inductance in Eq. (8) is constant, due to assumed linearity of the magnetic circuit. Index σ in Eqs. (6) and (7) denotes leakage inductances of stator and rotor.

Terms of the form $\omega\psi$ in Eqs. (4) and (5) are already mentioned fictitious electromotive forces that represent relative motion between stator and rotor phase windings, as well as the relative motion between all the phase windings and the common d–q reference frame.

Taking mechanical power as positive in motoring, the equation of mechanical motion is

$$T_e - T_L = \frac{J}{P}\frac{d\omega}{dt} \tag{9}$$

where J, P, and T_L stand for inertia, number of pole pairs, and load torque, respectively; mechanical angular speed is ω/P; friction is neglected; and electromagnetic torque is given by

$$\begin{aligned} T_e &= \frac{3}{2}P(\psi_{ds}i_{qs} - \psi_{qs}i_{ds}) = \frac{3}{2}P\frac{L_m}{L_r}(\psi_{dr}i_{qs} - \psi_{qr}i_{ds}) \\ &= \frac{3}{2}P(\psi_{dm}i_{qs} - \psi_{qm}i_{ds}) \end{aligned} \tag{10}$$

Coefficient $\frac{3}{2}$ in the torque expression is a consequence of the power correlation between the original and the equivalent induction machine. Inverse correlation between d-q-axis variables and original phase domain variables is established in the same way for voltages, currents, and flux linkages. For example, for stator quantities

$$\begin{aligned} f_a &= f_{ds}\cos\theta_s - f_{qs}\sin\theta_s \\ f_b &= f_{ds}\cos(\theta_s - 2\pi/3) - f_{qs}\sin(\theta_s - 2\pi/3) \\ f_c &= f_{ds}\cos(\theta_s - 4\pi/3) - f_{qs}\sin(\theta_s - 4\pi/3) \end{aligned} \tag{11}$$

Transformation expressions of the same form, with appropriate change of indices, apply to rotor variables.

Equations (1), (2), and (4) through (11), together with definitions of various spatial angles, completely describe an induction machine in an arbitrary common reference frame. All the variables and parameters of the rotor winding are referred to the stator by means of turns ratio. The model in an arbitrary reference frame yields an appropriate model for any specified value of the common reference frame angular speed. In the special case when $\omega_a = 0$, equations in a stationary α, β reference frame result:

$$\begin{aligned} v_{\alpha s} &= R_s i_{\alpha s} + \frac{d\psi_{\alpha s}}{dt} \\ v_{\beta s} &= R_s i_{\beta s} + \frac{d\psi_{\beta s}}{dt} \end{aligned} \tag{12}$$

$$\begin{aligned} v_{\alpha r} = 0 &= R_r i_{\alpha r} + \frac{d\psi_{\alpha r}}{dt} + \omega\psi_{\beta r} \\ v_{\beta r} = 0 &= R_r i_{\beta r} + \frac{d\psi_{\beta r}}{dt} - \omega\psi_{\alpha r} \end{aligned} \tag{13}$$

Equations (1), (2), and (11) remain valid, with change of indices, $d \to \alpha$ and $q \to \beta$, and provided that it is recognized that $\omega_a = 0$ means $\theta_s = 0$ and $\theta_r = -\theta$. Equations (3), (6)–(8), and (10) remain unaltered, with change of indices $d \to \alpha$ and $q \to \beta$. Equation (9) is unchanged.

Complex Space Vector Model

A mathematical model of an induction machine in terms of real d-q-axis variables, expressed in an arbitrary reference frame, contains for each variable (voltage, current, flux linkage of either stator or rotor) two components that are mutually perpendicular. This is a consequence of the 90° displacement between the d-axis and the q-axis. It is possible to regard the d-q reference frame as an orthogonal rotating system of axes in which a variable along one axis represents a real part of a complex variable, while the same variable along the other axis represents the imaginary part of the complex variable. So defined complex numbers are called space vectors (4, 7).

It is convenient to define space vectors initially in a stationary reference frame. Components along the α, β axes of both stator voltage and current are correlated with phase quantities by Eq. (1), with angle θ_s set to zero. The stator voltage space vector and stator current space vector are defined in the stationary reference frame as follows (symbols for space vectors are in boldface italic, while the superscript s denotes the stationary reference frame):

$$\begin{aligned} \boldsymbol{v}_s^s &= v_{\alpha s} + jv_{\beta s} = v_s e^{j\beta_s} \\ \boldsymbol{i}_s^s &= i_{\alpha s} + ji_{\beta s} = i_s e^{j\epsilon_s} \end{aligned} \tag{14}$$

where both, being complex numbers, are expressed in polar form as well. As α, β components of both voltage and current are time-varying quantities, the phase of both complex numbers is a time-varying quantity. If transformation expressions for α, β components, Eq. (1) with θ_s set to zero, are substituted in Eq. (14), correlation between space vectors in stationary reference frame and actual phase variables is obtained

$$\begin{aligned} \boldsymbol{v}_s^s &= \frac{2}{3}(v_a + \boldsymbol{a}v_b + \boldsymbol{a}^2 v_c) \\ \boldsymbol{i}_s^s &= \frac{2}{3}(i_a + \boldsymbol{a}i_b + \boldsymbol{a}^2 i_c) \end{aligned} \tag{15}$$

where $a = e^{j2\pi/3}$ is a spatial operator. To express a space vector in an arbitrary reference frame, it is necessary to rotate the space vectors of Eq. (15) for an angle that defines an instantaneous position of the d-axis of the common reference frame with respect to the stationary phase a-axis. Stator voltage and current space vectors are given in an arbitrary reference frame with

$$\begin{aligned} \boldsymbol{v}_s &= \boldsymbol{v}_s^s e^{-j\theta_s} \\ \boldsymbol{i}_s &= \boldsymbol{i}_s^s e^{-j\theta_s} \end{aligned} \tag{16}$$

Substitution of Eq. (14) in Eq. (16) yields

$$\begin{aligned} \boldsymbol{v}_s &= v_{ds} + jv_{qs} = v_s e^{j(\beta_s - \theta_s)} \\ \boldsymbol{i}_s &= i_{ds} + ji_{qs} = i_s e^{j(\epsilon_s - \theta_s)} \end{aligned} \tag{17}$$

Manipulation of Eqs. (4)–(8) enables creation of the complex, space vector model of an induction machine (7):

$$\begin{aligned} \boldsymbol{v}_s &= R_s\boldsymbol{i}_s + \frac{d\boldsymbol{\psi}_s}{dt} + j\omega_a\boldsymbol{\psi}_s \\ 0 &= R_r\boldsymbol{i}_r + \frac{d\boldsymbol{\psi}_r}{dt} + j(\omega_a - \omega)\boldsymbol{\psi}_r \end{aligned} \tag{18}$$

$$\begin{aligned} \boldsymbol{\psi}_s &= L_s\boldsymbol{i}_s + L_m\boldsymbol{i}_r = L_{\sigma s}\boldsymbol{i}_s + \boldsymbol{\psi}_m \\ \boldsymbol{\psi}_r &= L_r\boldsymbol{i}_r + L_m\boldsymbol{i}_s = L_{\sigma r}\boldsymbol{i}_r + \boldsymbol{\psi}_m \\ \boldsymbol{\psi}_m &= L_m\boldsymbol{i}_m \\ \boldsymbol{i}_m &= \boldsymbol{i}_s + \boldsymbol{i}_r \end{aligned} \tag{19}$$

where the remaining space vectors are defined as

$$\begin{aligned}
&\boldsymbol{\psi}_s = \psi_s e^{j(\phi_s-\theta_s)}: \quad \psi_r = \psi_r e^{j(\phi_r-\theta_s)}: \quad \boldsymbol{i}_r = i_r e^{j(\epsilon_r-\theta_s)}\\
&\boldsymbol{\psi}_s^s = \psi_s e^{j\phi_s}: \quad \psi_r^s = \psi_r e^{j\phi_r}: \quad i_r^s = i_r e^{j\epsilon_r}\\
&\psi_m = \psi_m e^{j(\phi_m-\theta_s)}: \quad i_m = i_m e^{j(\phi_m-\theta_s)}\\
&\psi_m^s = \psi_m e^{j\phi_m}: \quad i_m^s = i_m e^{j\phi_m}
\end{aligned} \tag{20}$$

Equation (9) remains unchanged. Electromagnetic torque and input power, Eqs. (10) and (3), can be given as

$$\begin{aligned}
&T_e = \frac{3}{2}P\,\mathrm{Im}\{\boldsymbol{i}_s\boldsymbol{\psi}_s^*\} = \frac{3}{2}P\frac{L_m}{L_r}\,\mathrm{Im}\{\boldsymbol{i}_s\boldsymbol{\psi}_r^*\} = \frac{3}{2}P\,\mathrm{Im}\{\boldsymbol{i}_s\boldsymbol{\psi}_m^*\}\\
&P_e = \frac{3}{2}\mathrm{Re}(\boldsymbol{v}_s\boldsymbol{i}_s^*)
\end{aligned} \tag{21}$$

where the symbol $*$ denotes complex conjugation. Equations (9), (18), (19) and (21) constitute, together with the appropriate transformation expressions, the complete complex space vector model of an induction machine.

PRINCIPLES OF VECTOR CONTROL OF INDUCTION MACHINES

The clue for decoupled flux and torque control in an induction machine lies in the choice of the common reference frame in which the machine is represented. The reference frame can be selected as firmly fixed to any of the three flux space vectors (stator, air-gap, and rotor flux) in the machine. The idea of field-oriented control requires that instantaneous values of the magnitude and spatial position of the stator current space vector with respect to the selected flux space vector in the machine can be controlled [i.e., that the stator current space vector is oriented with respect to the chosen flux space vector (4)]. Because in an induction machine there exist three flux space vectors [Eq. (20)], it is possible to realize stator flux oriented, rotor flux oriented and air-gap flux oriented control (1, 4, 5). The requirement for instantaneous control of the magnitude and spatial position of the stator current space vector translates itself into the requirement that amplitude, frequency, and phase of stator phase currents have to be instantaneously controllable (8).

The induction machine is fed from a power electronic converter with closed-loop current control in vector-controlled drives. The converter is usually a voltage source inverter operated in the pulse-width modulated (*PWM*) mode. Stator voltages are obtained on the basis of the closed-loop current control, so that the machine is fed from a current regulated PWM (*CRPWM*) voltage source inverter. It is possible to view an induction machine in two different ways, depending on the selected current control method. If closed-loop current control is performed using actual phase currents (current control in a stationary reference frame), it is possible to regard an induction machine as current fed. Reference stator phase currents are equal to actual phase currents under ideal conditions, and it may be assumed that the currents rather than the voltages are impressed into the machine's stator winding. Stator currents are thus known and stator voltage equations may be omitted from consideration. In contrast to this, if closed-loop current control is performed using transformed d-q-axis stator current components (current control in rotational reference frame), the machine cannot be regarded as current fed and stator voltage equations have to be considered. In this case a voltage-fed machine results (3, 5, 9). (It should, however, be noted that the voltage source is still current-controlled.)

Rotor flux oriented control yields the simplest configuration of the control system and is therefore the most frequently applied method. Although rotor flux oriented control is utilized in conjunction with both current-fed and voltage-fed machines, the analysis is here restricted to the simpler of the two (i.e., to rotor flux oriented control of a current-fed induction machine).

Rotor Flux Oriented Control of a Current-Fed Induction Machine

Consider the space vector model of an induction machine, [Eqs. (18)–(21)]. The machine is assumed to be current fed and stator voltage equation is therefore omitted. Let the common reference frame be fixed to the rotor flux space vector and, moreover, let the d-axis (real axis) of this common reference frame coincide with the rotor flux space vector. Then

$$\begin{aligned}
&\theta_s = \phi_r\\
&\theta_r = \phi_r - \theta\\
&\omega_s = \omega_r\\
&\omega_r = d\phi_r/dt
\end{aligned} \tag{22}$$

The rotor flux space vector of Eq. (20) is a real variable in this reference frame:

$$\begin{aligned}
&\boldsymbol{\psi}_r = \psi_{dr} + j\psi_{qr} = \psi_r\\
&\psi_{qr} = 0\\
&d\psi_{qr}/dt = 0\\
&\psi_{dr} = \psi_r
\end{aligned} \tag{23}$$

Figure 1 illustrates rotor flux and stator current space vectors in this special common reference frame.

Consider now electromagnetic torque expressed in terms of the rotor flux space vector, Eq. (21). Taking into account Eq. (23), Eq. (21) yields

$$T_e = \frac{3}{2}P\frac{L_m}{L_r}\psi_r\,\mathrm{Im}\{\boldsymbol{i}_s\} = \frac{3}{2}P\frac{L_m}{L_r}\psi_r i_{qs} \tag{24}$$

The torque equation is of the same form as in a separately excited dc machine and, if magnitude of the rotor flux is kept constant, torque can be controlled solely by stator q-axis current.

To accommodate the rotor voltage equation of Eq. (18) to the chosen reference frame, rotor current space vector has to be expressed from Eq. (19) using Eq. (23):

$$\boldsymbol{i}_r = (\psi_r - L_m\boldsymbol{i}_s)/L_r \tag{25}$$

Substitution of Eq. (25) into Eq. (18), with Eq. (22) accounted for, results in the following complex rotor voltage equation (rotor time constant is introduced as $T_r = L_r/R_r$):

$$0 = \frac{1}{T_r}\psi_r + \frac{d\psi_r}{dt} + j(\omega_r - \omega)\psi_r - \frac{1}{T_r}L_m\boldsymbol{i}_s \tag{26}$$

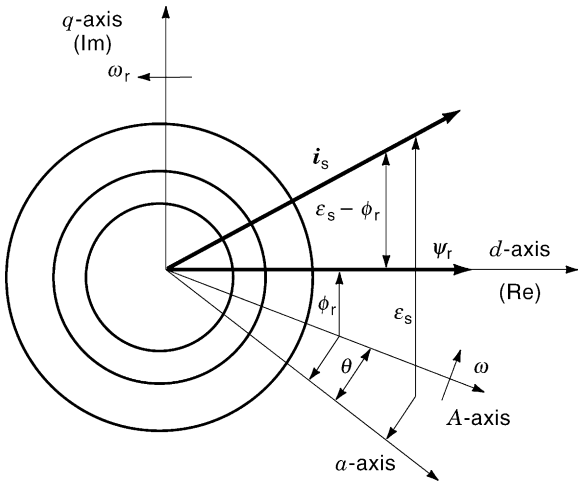

Figure 1. Rotor flux and stator current space vectors in the common d-q reference frame fixed to the rotor flux space vector. Rotor flux space vector is aligned with d-axis of the reference frame at all times, and speed of rotation of the two is the same.

Separation of Eq. (26) into real and imaginary parts yields

$$\psi_r + T_r \frac{d\psi_r}{dt} = L_m i_{ds} \tag{27}$$

$$(\omega_r - \omega)\psi_r T_r = L_m i_{qs} \tag{28}$$

Equation (27) reveals that the magnitude of the rotor flux can be controlled by the stator d-axis current and that it is constant if the stator d-axis current is constant. According to Eq. (28), the angular slip frequency $\omega_{sl} = \omega_r - \omega$ linearly depends on the stator q-axis current when the magnitude of rotor flux is constant. Developed torque is then proportional to slip frequency. If the stator d-axis current is constant, rotor flux is constant and torque can be instantaneously altered if it is possible to change the stator q-axis current instantaneously. If the machine is current fed, Eqs. (24), (27), and (28) constitute the complete model. Thus decoupled torque and flux control can be obtained with a current-fed machine, provided that the control system operates in the rotor flux oriented reference frame. The machine is, however, supplied with three-phase ac currents. It is therefore necessary to include a coordinate transformation between the controller and the power supply.

Coordinate transformation requires information on the instantaneous position of the rotor flux space vector. The schemes of rotor flux oriented control may be subdivided into two groups, depending on how this information is obtained. In indirect schemes the position of the rotor flux space vector is calculated without the use of measured electromagnetic variables. In direct control schemes some measured electromagnetic variables are used for rotor flux position calculation.

Direct Rotor Flux Oriented Control of an Induction Machine

Figure 2 illustrates control system of a current-fed direct rotor flux oriented induction machine, which comprises a

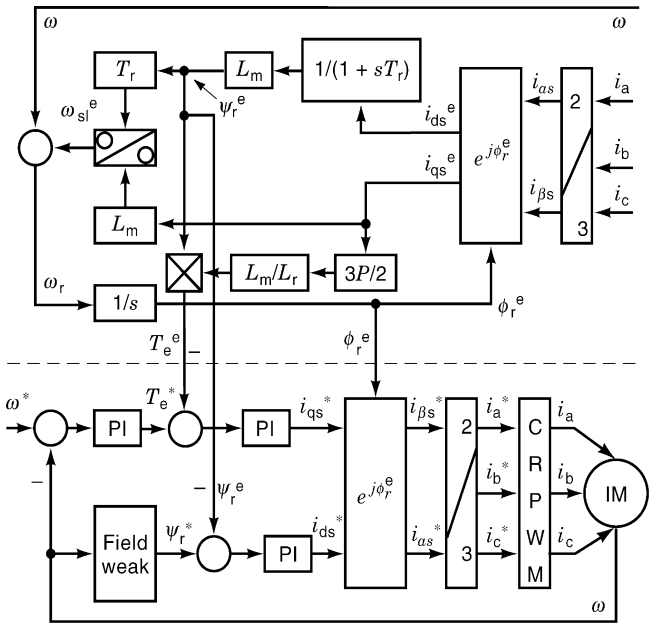

Figure 2. Control system of a current-fed direct rotor flux oriented induction machine. Stator d-q-axis current references are created by two independent control loops operating in parallel and are converted into phase current references by means of a coordinate transformation. Estimation of the rotor flux space vector is performed using measured stator currents and rotor speed. The estimator operates in the rotor flux oriented reference frame, and measured stator currents have to be transformed using inverse coordinate transformation.

rotor flux (PI) controller, speed (PI) controller, and torque (PI) controller. The information regarding rotor flux position and amplitude (and torque) is obtained from measured signals, as discussed shortly. The two control paths that generate stator d-q-axis current references operate in parallel, independently one of the other. An asterisk denotes reference (commanded) quantities, while a superscript e stands for estimated variables. Feedback signals include rotor speed (which is measured or calculated from measured rotor position) and measured stator currents. The CRPWM inverter is assumed to be ideal, so that reference and actual stator phase currents are equal. The two transformation blocks between d-q-axis currents and phase current references describe the coordinate transformation of Eq. (11), performed in two steps as discussed in conjunction with Eq. (1). The outputs of the speed and rotor flux controllers are limited and the provision for field weakening is included. The field-weakening block keeps rotor flux at a constant rated value in the base speed region (up to the rated speed) and reduces rotor flux reference inversely proportionally to the speed above base speed. Such a change of rotor flux reference is frequently applied although it is simplified with respect to the optimal rotor flux reference change in the field weakening region (1, 10).

Rotor flux estimation in direct schemes of rotor flux oriented control can be performed in various ways. Air-gap (main, magnetizing) flux, stator currents, stator voltages, and rotor speed (position) are measurable quantities, and different combinations of these signals can be used (11).

The method based on stator current and air-gap flux measurement performs calculations using Eqs. (6) and (7) in a stationary reference frame. It requires installation of flux sensors or tapping of stator windings (11) and is rarely applied today. The second method asks for measurement of stator voltages and stator currents (12), and the magnitude and position of the rotor flux space vector are calculated from Eqs. (12), (6), and (7) in the stationary reference frame. The method involves integration, and estimation becomes inaccurate at low speeds.

A frequently utilized method of rotor flux space vector estimation, shown in the upper part of Fig. 2, uses measured stator currents and rotor speed (9) (it will be denoted as $i_s - \omega$ estimator). The main advantages of this scheme are that there is no need for special construction or modification of the machine, integration of voltages is avoided, and estimation is operational at zero speed. It is used in the vector control system of Fig. 2 and in rotor flux oriented voltage-fed induction machines with current control in the rotational reference frame (9). The estimator performs calculations on the basis of the model of an induction machine in a rotor flux oriented reference frame [Eqs. (24), (27), and (28)]. Rotor flux position is calculated by integrating the sum of the measured rotor speed and estimated angular slip frequency, as shown in Fig. 2, where symbol s denotes the Laplace operator. Measured stator currents have to be transformed into a rotor flux oriented reference frame. The major shortcoming of this method is the strong dependence of estimation accuracy on parameter variation effects. The same remark applies to indirect rotor flux oriented control, which is discussed next.

Indirect Rotor Flux Oriented Control of an Induction Machine

If the rotor flux space vector position is calculated in a feedforward manner, using measured speed (position) and references rather than measured electromagnetic variables, indirect rotor flux oriented control results (current measurement remains necessary in order to establish closed-loop current control). Equations (24), (27), and (28) enable calculation of the reference stator d-q-axis current components, reference angular slip speed, and desired rotor flux spatial position as follows (1):

$$\begin{aligned} i_{qs}^{*} &= \frac{2}{3P}\frac{T_e^{*}}{\psi_r^{*}}\frac{L_r}{L_m} \\ i_{ds}^{*} &= \frac{1}{L_m}\left(\psi_r^{*} + T_r\frac{d\psi_r^{*}}{dt}\right) \end{aligned} \tag{29}$$

$$\begin{aligned} \omega_{sl}^{*} &= \frac{L_m}{T_r}\frac{i_{qs}^{*}}{\psi_r^{*}} \\ \phi_r^{e} &= \int (\omega_{sl}^{*} + \omega)\, dt \end{aligned} \tag{30}$$

Figure 3 shows an indirect rotor flux controller, based on Eqs. (29) and (30) (an asterisk again denotes reference quantities). Prevailing applications are for drives that require operation in the base speed region only (where rotor flux reference is constant and rated) and it is then possible to simplify the control scheme. Such a drive is shown in the lower part of Fig. 3, where due to ψ^{*}_r = const., $i^{*}_{ds} = \psi^{*}_r/L_m$ is constant as well. Torque command is obtained as output from the speed PI controller. Indirect vector control is a frequent choice in practical realizations as the control system is significantly simpler, compared to direct orientation schemes.

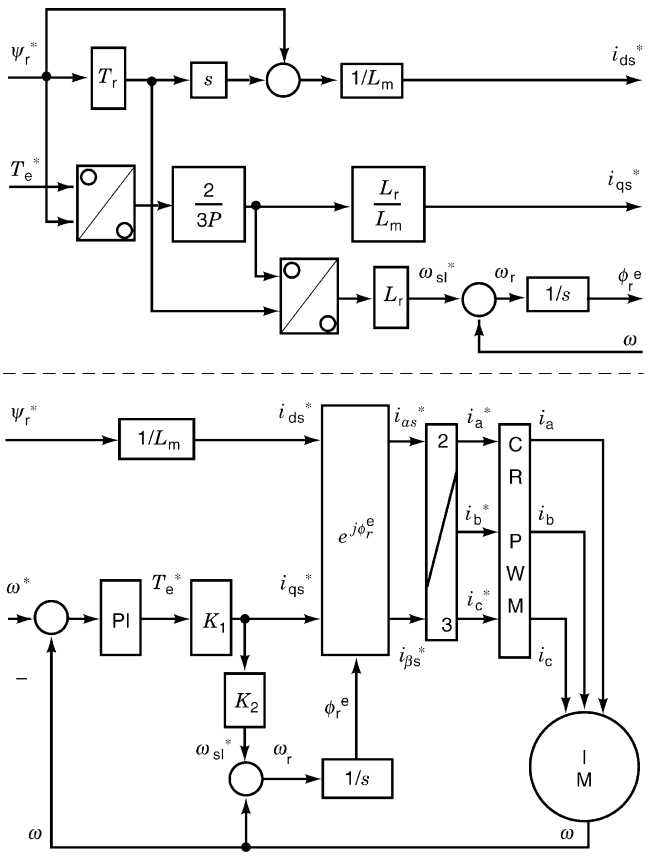

Figure 3. Outlay of an indirect rotor flux oriented controller and its implementation in conjunction with a current-fed induction machine for operation in the base speed (constant flux) region [$K_1 = (2/3P)(L_r/L^2{}_m)/i^*_{ds}$, $K_2 = 1/(T_r i^*_{ds})$].

Performance of a Rotor Flux Oriented Induction Machine

Dynamic performance of a rotor flux oriented induction machine is most easily examined using simulations. Simulation programs must include representation of the control system and an appropriate model of the induction machine. A power electronic converter can be omitted from the simulation if performance is analyzed under ideal supply conditions. The most appropriate model of the induction machine is then the one given by Eqs. (4)–(10), formed in the reference frame fixed to the rotor flux space vector angular speed determined by the control system. Such an approach enables omission of the coordinate transformation blocks, as outputs of the control system become directly inputs into the machine model. Stator voltage equations are not required when a current-fed machine is analyzed. Note that the motor model must include an equation for the time derivative of the rotor flux q-axis component. If rotor flux oriented control is achieved, simulation will give rotor flux along the q-axis as equal to zero.

If a current-controlled PWM voltage source inverter is included in the simulation model, it is most convenient to represent the induction machine in the stationary reference frame. Stator voltage equations now have to be included in the model.

Figure 4 presents a simulation illustration of dynamics of a rotor flux oriented induction machine. The results apply to the direct rotor flux oriented induction machine of Fig. 2. All the parameters of the estimator are taken as equal to those in the machine model and the operation is simulated assuming ideal current feeding (i.e., the model does not include inverter representation, the machine is represented with d-q-axis model in the reference frame fixed to the estimated rotor flux position, and stator current commands are inputs into the machine model so that stator voltage equations are omitted). All the three controllers of Fig. 2 are of PI type, so that in any steady-state operation reference and actual speed are equal, as are the estimated and reference torque and rotor flux. The machine initially operates in steady state with rated rotor flux command, zero load torque, and speed equal to 40% of the rated in negative direction of rotation. Speed reversal is then initiated with a ramplike speed reference change, from −40% to +40% of the rated speed. Rotor flux reference remains rated. Change in speed command leads to fast buildup of the stator q-axis current, leading to a corresponding buildup of torque of the same profile. Actual and estimated torque values coincide. Maximum torque is limited to seven times rated. No change in rotor flux takes place, stator d-axis current remains the same as before the transient, and decoupled control of flux and torque is achieved. The final steady state is identical to the original one, except that the machine rotates in the positive direction.

Another important feature of the drive is its response to a sudden application and removal of the load torque. Figure 5 shows transients that now take place. It is an experimental recording of the operation of an indirect rotor flux oriented induction machine of the structure illustrated in Fig. 3 (index n stands for rated values). The machine initially operates with 70% of the rated rotor flux (70% of the rated stator d-axis current) at a speed of 600 rpm under no-load conditions. Step load torque is at first applied and then removed. Stator q-axis current command and the measured speed are shown. Speed initially drops following the application of the load torque. Torque quickly builds up and returns speed to the reference value. Removal of the load torque has the opposite effect. Speed initially exceeds reference, causing rapid reduction in the torque, which leads to return of the speed to the reference value.

Simulation and experimental results in Figs. 4 and 5 show that rotor flux oriented control is indeed characterized by very quick torque response. Torque response is smooth, without any unwanted oscillations, so that speed change is uniform and as rapid as possible.

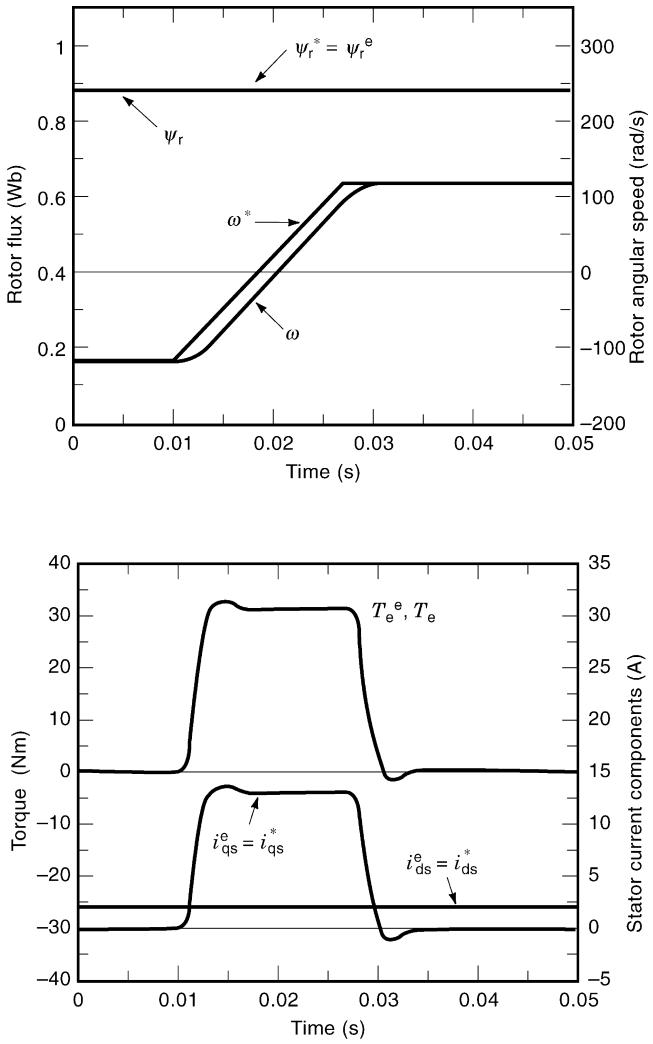

Figure 4. Speed reversal of a current-fed direct rotor flux oriented induction machine in the base speed region (simulation, 0.75 kW machine). Torque builds up rapidly, and interaction between d- and q-axes does not take place, as witnessed by the unchanged value of the rotor flux in the machine. Decoupled rotor flux and torque control is thus achieved.

Other Orientation Possibilities

As already noted, rotor flux oriented control can be realized with closed-loop current control of stator d-q-axis current components, resulting in a voltage-fed machine. The model derived for a rotor flux oriented current-fed induction machine remains valid. However, stator voltage equations now have to be considered and outputs of the control system are now references for stator voltage d-q-axis components rather than references for stator current components. Correlation between stator d-q-axis voltages and stator d-q-axis currents is not decoupled, and it is necessary to include a decoupling circuit in the control system, which decouples stator voltages and currents along d-q-axes (9). The resultant control structure is more complex than the one of a current-fed machine.

It is possible to realize vector control with stator current orientation along stator flux and along air-gap flux space vectors (4). If the derivation procedure for a current-fed machine is done for stator flux and air-gap flux oriented control, the main reason for predominant use of rotor flux oriented control becomes obvious. The models of a current-fed machine in these two reference frames do not possess

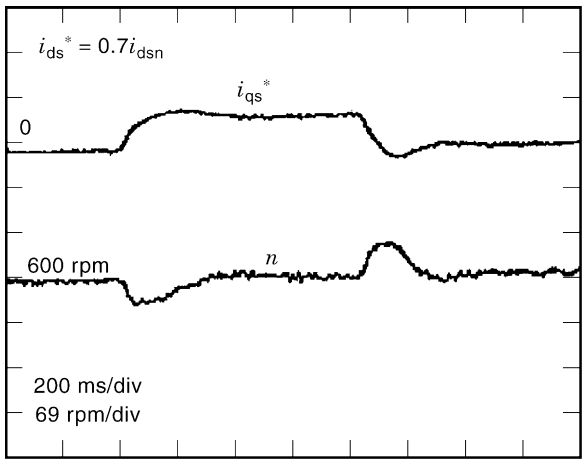

Figure 5. Step loading and unloading of an indirect rotor flux oriented induction machine (experiment, 0.75 kW machine). Application and removal of the load torque initiate rapid torque response, which returns the speed to the reference value.

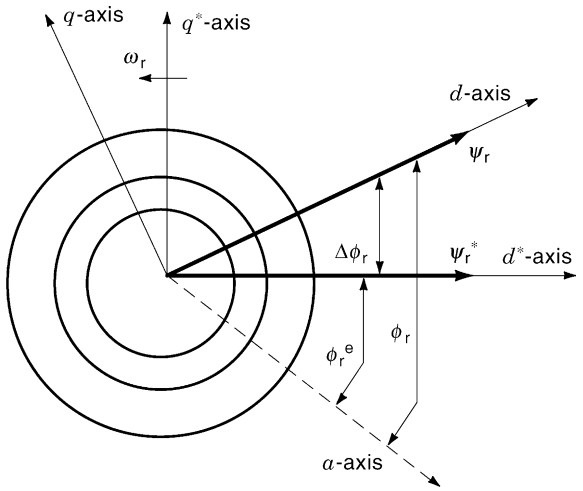

Figure 6. Illustration of commanded (d^*-q^*) and actual (d-q) rotor flux oriented reference frames in detuned operation. Because the commanded reference frame does not coincide with the actual one, decoupled rotor flux and torque control does not take place.

the main feature of rotor flux oriented control—namely, that flux and torque can be independently controlled by two stator current components in a decoupled manner. The equations are coupled and it is therefore necessary to introduce decoupling circuits into the control system even when the machine is current fed (13). Decoupling circuits significantly increase the complexity of the drive.

As a result of existence of three types of vector control (orientation along rotor, air-gap and stator flux), which each can be realized using either indirect or direct vector control, so-called "universal field oriented controller" has been introduced (14). This controller can operate in any of the three reference frames, with either indirect or direct type of control, and various operating modes can be used in different speed regions, with smooth changeover during operation of the machine (15).

PARAMETER VARIATION EFFECTS IN ROTOR FLUX ORIENTED INDUCTION MACHINES

The constant parameter model of an induction machine is used for calculation of rotor flux space vector position in both direct and indirect vector control schemes. If the value of any of the parameters in the control part differs from the corresponding actual value in the machine, so-called detuning occurs. This means that the estimated rotor flux position, calculated by the controller and used for coordinate transformation, does not correspond to the actual rotor flux position in the machine, so that field orientation is not achieved. Figure 6 illustrates detuned operation; the d-q-axis reference frame determined by the controller is denoted with an asterisk. The actual rotor flux space vector is displaced from the d-axis of this reference frame, so that the actual rotor flux oriented d-q reference frame does not coincide with the frame assumed by the controller. The consequence of detuning is that decoupled rotor flux and torque control does not take place, and this leads to unwanted transients in torque response and to steady-state errors in both rotor flux and torque.

Induction machine parameters are subject to variation due to various reasons. Stator and rotor resistance change with operating temperature. Stator and rotor leakage inductance vary due to different levels of saturation of the leakage flux paths. Magnetizing inductance varies with changes in the saturation level of the main flux path. Rotor resistance and rotor leakage inductance may change with rotor frequency due to skin effect. Iron losses are often neglected in the model of the induction machine from which vector control principles are derived.

A variety of schemes of rotor flux oriented control make a unified analysis of performance deterioration due to parameter variation effects impossible. Different schemes rely on the use of different parameters in a different way. The analysis of parameter variation effects is here restricted to a current-fed machine with control schemes of Figs. 2 and 3. The reason for this specific selection is twofold. First, these two types of rotor flux orientation are most frequently utilized. Second, as both of these schemes rely on the same equations for achieving field orientation [Eqs. (29) and (30) for the indirect scheme and Eqs. (24), (27), and (28) for the direct scheme], their steady-state behavior under detuned conditions is identical. Thus the following steady-state analysis of detuned operation applies to the both schemes. Stator resistance and stator leakage inductance are not involved in the rotor flux position calculation. Hence their variations have no impact on operation of the drive and can be excluded from further analysis.

Rotor resistance and rotor leakage inductance vary with rotor frequency only in deep-bar and double-cage induction machines (16). Variation of rotor leakage inductance due to saturation of the rotor leakage flux path is a secondary order effect (17), as rotor leakage inductance enters all the controller equations summed with the magnetizing inductance, which is 10 to 100 times greater. Omission of iron loss representation in the vector controller leads to detuning that is relatively small (18, 19). These considerations leave two sources of detuning as most relevant: main flux

saturation and temperature-related variation in rotor resistance.

Main Flux Saturation

Induction machines are designed to operate around the knee of the non-linear magnetizing curve. Magnetizing flux and magnetizing inductance have rated values (denoted with index n) in the rated operating point on this curve. If the magnetizing flux is changed from rated value in either direction, the value of the magnetizing inductance will change. Non-linearity of the magnetizing curve has numerous consequences on the operation of a vector controlled induction machine. It affects available torque per ampere and needs to be accounted for if this ratio is to be maximized in steady-state and/or transient operation (1, 20). Developed torque and its linearity are affected as well (1, 21). Next, there are numerous situations when rotor flux reference, and hence the main flux saturation level as well, are altered dynamically during operation of the drive. When speed exceeds rated value, the machine operates in the field-weakening region and rotor flux reference is reduced below rated. Since a reduction of flux reference leads to an increase in the magnetizing inductance, non-linearity of the magnetizing curve has to be taken into account (22). Rotor flux oriented control is well suited to operation of an induction machine with optimal efficiency. In this case rotor flux reference is varied until input power consumption reaches minimum for a given load. When the load is light, optimal efficiency is achieved with reduced flux (23). Thus, depending on the operating cycle of the machine, continuous variation of the reference rotor flux takes place although the machine may operate in the base speed region only. Variation of rotor flux reference changes magnetizing inductance, so that accuracy of field orientation is affected. Optimal efficiency control, as applied in vector controlled induction motor drives, is considered later on in this article in more detail.

Steady-state analysis of detuning due to main flux saturation requires incorporation of the magnetizing curve into the steady-state model (1, 21). The analysis is done in the d-q reference frame determined by the controller (d^*-q^* reference frame of Fig. 6). Steady-state operation of the indirect vector controller (Fig. 3) is described by

$$\begin{aligned} i^*_{ds} &= \psi^*_r / L^*_m & i^*_{qs} &= T^*_e / \psi^*_r (L^*_r / L^*_m)(1/K) \\ \omega^*_{sl} &= (L^*_m i^*_{qs})/(T^*_r \psi^*_r) & \phi^e_r &= \int (\omega^*_{sl} + \omega)\, dt = \int \omega_r\, dt \\ \omega^* &= \omega & T_e &= T_L \end{aligned} \tag{31}$$

Equality of reference and actual speed is a consequence of the action of the PI speed controller, which forces steady-state speed error to zero. Actual torque developed by the machine equals load torque. In Eq. (31) and in what follows, apart from reference values, an asterisk denotes parameter values used in the controller. Constant K stands for $(\frac{3}{2})P$.

Consider next Eqs. (5) and (10). Elimination of rotor current components by means of Eq. (7), formulation of the equations in the reference frame dictated by the controller, and application of the steady-state constraint $d/dt = 0$ lead to the following equations:

$$\begin{aligned} (1/T_r)\psi_{dr} &= (L_m/T_r) i^*_{ds} + \omega^*_{sl} \psi_{qr} \\ (1/T_r)\psi_{qr} &= (L_m/T_r) i^*_{qs} - \omega^*_{sl} \psi_{dr} \\ T_e &= K(L_m/L_r)(\psi_{dr} i^*_{qs} - \psi_{qr} i^*_{ds}) \end{aligned} \tag{32}$$

Stator current d-q-axis components and slip frequency in Eq. (32) equal reference values due to the choice of the reference frame and idealized treatment of the inverter. Magnetizing inductance in Eq. (32) in general differs from the one in Eq. (31). Hence rotor time constants differ as well. Let the ratio of magnetizing inductances be $\beta = L_m/L^*_m$. Then $\alpha = T_r/T^*_r = L_r/L^*_r = (\beta + \sigma_r)/(1 + \sigma_r)$, where $\sigma_r = L^*_{\sigma r}/L^*_m$ = constant. Steady-state detuning is characterized by three quantities: ratio of actual to commanded rotor flux, ratio of actual to commanded torque, and error in orientation angle. Magnitude of the actual rotor flux and error in the orientation angle are defined as

$$\begin{aligned} \psi_r &= \sqrt{\psi^2_{dr} + \psi^2_{qr}} \\ \Delta\phi_r &= \tan^{-1}(\psi_{qr}/\psi_{dr}) \end{aligned} \tag{33}$$

where actual rotor flux d-q-axis components are projections of the actual rotor flux space vector onto the d^*-q^* system of axes in Fig. 6. If Eq. (32) is solved for rotor flux d-q-axis components, these are further inserted into the torque equation of Eq. (32) and the controller equations [Eq. (31)] are then accounted for, detuning characteristics are obtained in the form

$$\begin{aligned} \frac{\psi_r}{\psi^*_r} &= \beta \sqrt{\frac{1 + (T^*_r \omega^*_{sl})^2}{1 + \alpha^2 (T^*_r \omega^*_{sl})^2}} \\ \frac{T_e}{T^*_e} &= \beta^2 \frac{1 + (T^*_r \omega^*_{sl})^2}{1 + \alpha^2 (T^*_r \omega^*_{sl})^2} = \left(\frac{\psi_r}{\psi^*_r}\right)^2 \\ \Delta\phi_r &= \tan^{-1}\left(\frac{(1-\alpha) T^*_r \omega^*_{sl}}{1 + \alpha (T^*_r \omega^*_{sl})^2}\right) \end{aligned} \tag{34}$$

Equation (34) can be used to assess trends in detuning due to saturation, by taking the ratio of magnetizing inductances β as an independent variable. However, to predict behavior of a given motor quantitatively, it is necessary to account for the actual magnetizing curve of the machine. Indeed, for the given rotor flux reference, torque reference, and magnetizing inductance in the controller, coefficient β is a dependent rather than independent variable, whose value is determined with the magnetizing curve:

$$\psi_m = f(i_m): \quad L_m = \psi_m / i_m = f_1(i_m) = f_2(\psi_m) \tag{35}$$

The procedure is iterative and encompasses Eqs. (7), (8), (34), and (35). The model derived so far is sufficient for characterization of the torque mode of operation (i.e., when speed control loop is open) as torque reference is taken as an independent input. In operation with closed-loop speed control, the equality of the load torque and machine's torque, given in Eq. (31), has to be satisfied. Due to detuning, reference torque does not equal actual torque and is, in general, unknown. If the product of the controller rotor time constant and reference slip frequency is expressed from Eq. (31) as $\omega^*_{sl} T^*_r = (1/K)(L^*_r/\psi^{*2}_r) T^*_e = h T^*_e$ and is

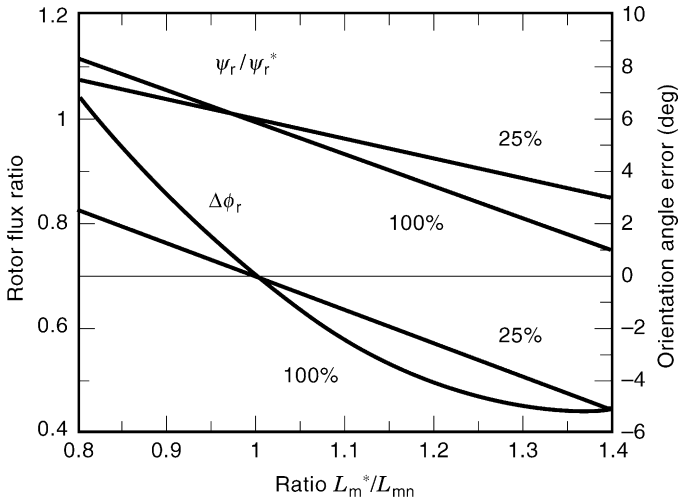

Figure 7. Orientation angle error and rotor flux ratio for incorrect setting of the magnetizing inductance in the controller (operation in the base speed region with rated rotor flux command, load torque as parameter, 4 kW machine). Error in the magnetizing inductance setting can lead to severe detuning.

then substituted into the torque ratio equation of Eq. (34), a third-order equation is obtained:

$$T_e^{*3} + T_e^{*2}\left(-\frac{\alpha^2}{\beta^2}T_L\right) + T_e^*\frac{1}{h^2} + \left(-T_L\frac{1}{\beta^2 h^2}\right) = 0 \qquad (36)$$

whose solution determines reference torque value. [Condition $T_e = T_L$ is accounted for in Eq. (36).] Coefficient h is a constant for given rotor flux reference and given value of the magnetizing inductance in the controller. Load torque is the independent variable in Eq. (36).

Figure 7 shows the steady-state detuning characteristics for the speed mode of operation (i.e., closed-loop speed control), for operation in the base speed region with constant rated rotor flux command. Load torque is the parameter, and characteristics are plotted against the ratio of magnetizing inductance in the controller to the rated magnetizing inductance value. Torque ratio, being equal to the rotor flux ratio squared, Eq. (34), is omitted. Detuning is independent of the speed, and characteristics show that incorrect setting of the magnetizing inductance in the controller can lead to severe orientation angle errors.

To investigate the dynamics of a saturated rotor flux oriented induction machine, a convenient dynamic saturated induction machine model is required. It is therefore necessary to modify the d-q-axis model given by Eqs. (4)–(7) by accounting for nonlinear correlation between magnetizing flux and magnetizing current in Eq. (8). State-space models of a saturated induction machine can be formed in various ways, depending on which variables are selected as state-space variables (24). Any of the dynamic saturated machine models may be used for simulation purposes. Furthermore, these models can be used to assess qualitatively the impact of main flux saturation on rotor flux oriented control. The net effect of main flux saturation is loss of decoupled rotor flux and torque control during transients and in steady states other than rated, even when the machine operates with rated constant rotor flux command and the value of magnetizing inductance in the controller equals rated (25). This is due to the fact that, according to Eq. (8), variation of stator q-axis current leads to variation of q-axis magnetizing current, so that the q-axis component of the magnetizing flux changes and causes alteration in the total magnetizing flux. Hence the magnetizing inductance varies as well. This effect is usually termed cross saturation and is insignificant in practice when torque is limited to at most twice the rated value (25). When the current-fed machine is analyzed, stator voltage equations can be omitted and stator d-q-axis current components and their derivatives then act as inputs to the model of the machine, which is formed in the reference frame fixed to the rotor flux position calculated by the controller.

Transient behavior is investigated for the direct rotor flux oriented current-fed induction machine of Fig. 2. The value of the magnetizing inductance in the estimator is set to rated and operation is simulated for the same reversing transient already depicted in Fig. 4. Figure 4 applies to an idealized situation when saturation is neglected, while the results, shown in Fig. 8, are obtained with saturation accounted for in the machine's model. As acceleration torque attains seven times the rated torque value, the q-axis component of the magnetizing current becomes significant and drives the machine into deep saturation. The flux estimator does not recognize this change in magnetic conditions, so that the rotor flux is erroneously estimated as remaining constant and equal to the reference value during the transient and the stator d-axis current command is kept unchanged. Actual torque is smaller than the estimated value. Speed response differs insignificantly from the one in Fig. 4 and is therefore not shown. Much the same behavior is observed if a change in saturation level takes place due to a change in rotor flux reference, which causes a change in stator d-axis current command (26). Thus it follows that even when the magnetizing inductance in the estimator (or indirect controller) is set to the rated value, there will be detuning if either significant cross saturation occurs or if the machine is operated with variable rotor flux command. If the magnetizing inductance value in the controller does not correspond to the rated (this situation is illustrated for steady states in Fig. 7), transient response deteriorates further.

Rotor Resistance Variation

Rotor resistance enters equations of both the indirect vector controller of Fig. 3 and the rotor flux estimator of Fig. 2 through the rotor time constant. The rotor time constant determines the accuracy of slip frequency calculation [Eqs. (28) and (30)]. As slip frequency is summed with rotor speed in order to calculate the position of the rotor flux space vector, any error in the value of the rotor resistance directly leads to detuned operation. The effects of variation in rotor resistance are analyzed in considerable depth in 27–29. An investigation of detuning due to rotor resistance variation has to be done in such a way that main flux saturation is included in the model of the machine (27–29). Thus the complete modeling procedure described in the previous subsection fully applies to the analysis of detuning due to rotor resistance variation. It is only necessary to set L^*_m

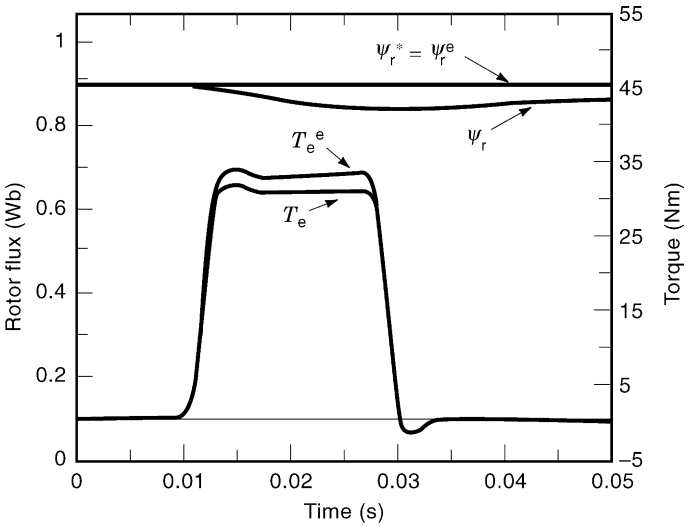

Figure 8. Influence of cross saturation on reversing transient (simulation, 0.75 kW machine). Actual rotor flux decreases, while rotor flux estimator erroneously judges flux as remaining constant. Developed transient torque is therefore smaller than the estimated torque. Speed response insignificantly differs from the one of Fig. 4, due to filtering action of the drive's inertia, and is therefore not shown.

to L_{mn}, define the ratio between the actual rotor resistance and the rotor resistance used in the controller as $r = R_r/R^*_r$, and take this coefficient as an independent variable. Introduction of this coefficient modifies detuning equations, so that detuning in the steady state with closed-loop speed control is described by

$$\frac{\psi_r}{\psi_r^*} = \beta \sqrt{\frac{1+(\omega_{sl}^* T_r^*)^2}{1+\left(\frac{\alpha}{r}\right)^2 (\omega_{sl}^* T_r^*)^2}}$$

$$\frac{T_e}{T_e^*} = \frac{\beta^2}{r} \frac{1+(\omega_{sl}^* T_r^*)^2}{1+\left(\frac{\alpha}{r}\right)^2 (\omega_{sl}^* T_r^*)^2} = \frac{1}{r}\left(\frac{\psi_r}{\psi_r^*}\right)^2 \tag{37}$$

$$\Delta\phi_r = \tan^{-1}\left(\frac{\omega_{sl}^* T_r^* \left(1-\frac{\alpha}{r}\right)}{1+\omega_{sl}^{*2} T_r^{*2} \frac{\alpha}{r}}\right)$$

$$T_e^{*3} + T_e^{*2}\left[-\left(\frac{\alpha}{\beta}\right)^2 \frac{1}{r} T_L\right] + T_e^* \frac{1}{h^2} + \left(-\frac{T_L}{h^2}\frac{r}{\beta^2}\right) = 0$$

Figure 9 displays steady-state detuning characteristics, which are again speed independent. The orientation angle error becomes significant for large discrepancies between actual and reference rotor resistance values.

Figure 10 illustrates transient operation with detuned rotor resistance. The scheme of Fig. 2 is simulated. The initial and final steady state correspond to operation with rated rotor flux, 80% of the rated speed, and zero load torque. The simulated transient is a step application and removal of the rated load torque. Two cases are shown: rotor resistance in the machine equal to 150% and 66%, respectively, of the value used in the controller. As the rotor flux estimator is unaware of the change in rotor resistance,

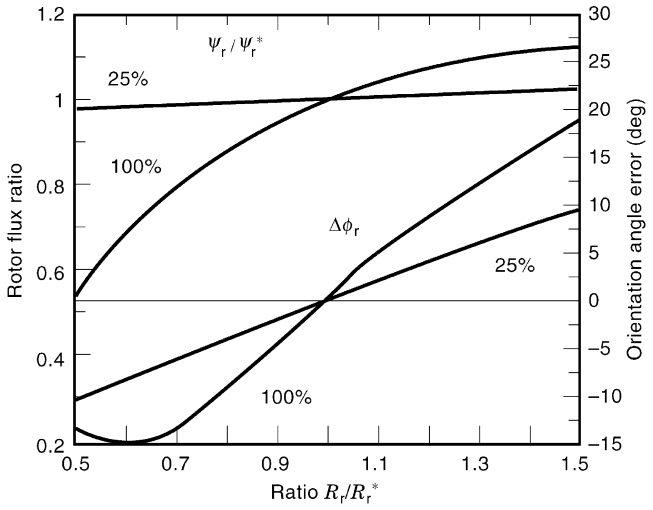

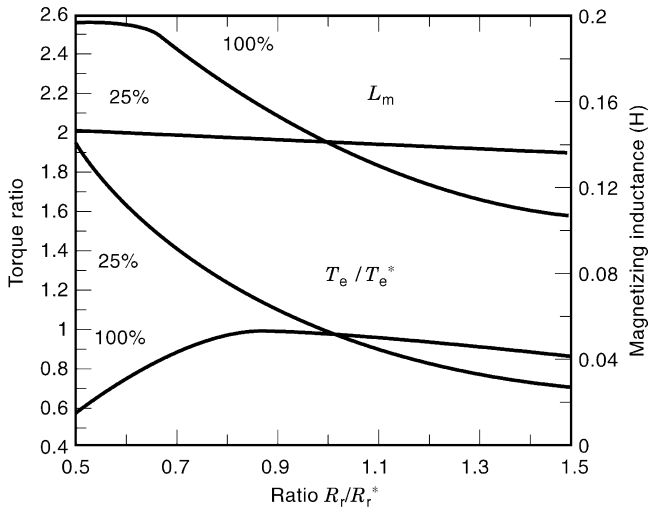

Figure 9. Steady-state detuning due to rotor resistance variation in the base speed region (rated rotor flux command, load torque as parameter, 4 kW machine). Detuning is speed independent but load dependent and is severe for large discrepancies between actual and reference rotor resistance values. Magnetizing inductance in the controller equals rated (0.141 H). Rotor resistance variation can cause significant change in the saturation level in the machine, as confirmed by magnetizing inductance variation in the machine for rated load torque operation.

estimated rotor flux in both cases equals commanded rotor flux. Actual torque developed by the machine equals applied load torque in steady state. However, estimated torque (which almost equals commanded torque in both transient and steady-state operation as the torque controller is very fast) significantly differs from the actual one. The same applies to the actual rotor flux. The actual rotor flux and estimated torque responses are oscillatory when rotor resistance in the machine is smaller than the one used in the controller. It should be noted that effects of rotor resistance detuning on transient performance are usually simulated in the torque mode of operation (i.e., with open speed control loop, 1, 27, 28), rather than with closed-loop

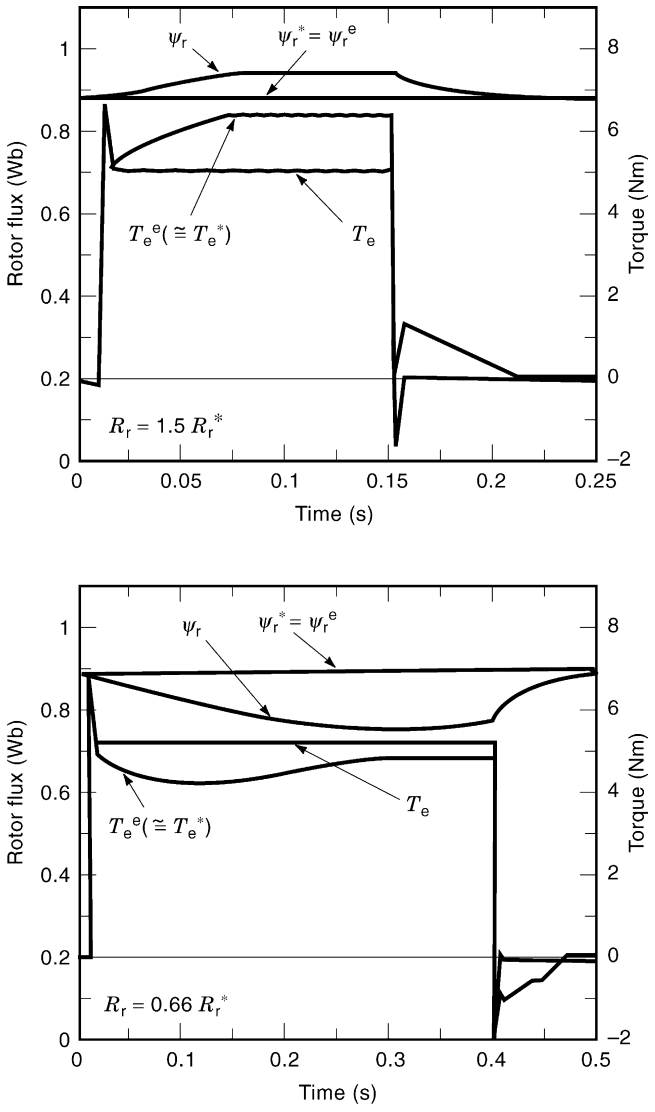

Figure 10. Illustration of detuning effects in transient operation caused by rotor resistance variation: responses to step loading and unloading with rated load torque for $R_r = 1.5R^*_r$ and $R_r = 0.66R^*_r$ (0.75 kW machine). Actual and estimated rotor flux and torque coincide when rotor resistance in the controller equals the one in the machine. However, with detuned rotor resistance only estimated rotor flux equals reference, while actual rotor flux deviates, causing a corresponding discrepancy between estimated and actual torques.

speed control, as it is done here. A step torque command is then applied as the input, and the behavior of the actual torque is observed. If such an approach is utilized, then actual torque in the machine essentially has the response obtained here for the estimated torque.

Results of presented detuning studies indicate the importance of initial correct setting of all the parameters used in the controller. Methods of experimental parameter identification are numerous (11) and an up-to-date survey is available in (30). Although a more detailed treatment of this topic is beyond the scope of interest here, an experimental method of magnetising curve identification (31) and one simple experimental method (32) of rotor time constant tuning in indirect vector control scheme of Fig. 3 are nevertheless described. Rotor time constant tuning is considered first.

Rotor flux command is set to rated value, so that the stator d-axis current command is rated. The machine is accelerated to a certain speed under no-load conditions and the speed loop is then opened. The machine further operates in torque mode and an alternating square-wave torque command, leading to the alternating square-wave q-axis stator current command, is applied. If the rotor time constant value in the controller is correct, the actual torque response is square wave. Square-wave torque, according to Eq. (9), causes a triangular variation of speed. If the rotor time constant value is incorrect, the actual torque is not a square-wave and the speed response deviates from triangular. Figure 11 depicts experimentally recorded speed response obtained with correct and incorrect rotor time constant setting. The machine operates with rated rotor flux command and with a square-wave rated torque (rated stator q-axis current) command. The deviation of speed response from triangular is evident when the value of rotor time constant is incorrect.

As already noted, one of the situations where variation in the level of main flux saturation becomes important is operation in the field weakening region. As the speed increases, rotor flux reference reduces, meaning that the machine's operating point on the magnetization curve moves towards the linear part. Hence the value of the magnetising inductance in the machine effectively increases, compared to the operation with rated rotor flux reference. In actual industrial drives, aimed at operation in both base speed region and the field weakening region, the indirect vector controller of Fig. 3 is often implemented in the form illustrated in Fig. 12 (mathematical procedure that enables derivation of this modified indirect vector controller is illustrated in the next section). Up to the base speed ω_B (usually rated speed) rotor flux reference is held at constant rated value (1 per unit). Rotor flux is weakened above base speed in inverse proportion to the speed. Compared to the full form shown in the upper part of Fig. 3, certain approximations are introduced. Rate of change of reference rotor flux is assumed to be small, since speed changes relatively slowly, so that derivative of rotor flux is neglected. This simplification also makes the magnetising flux equal to the rotor flux, while magnetising current becomes equal to the stator d-axis current (31). The input into the system is the rated stator d-axis current reference and the inverse magnetizing curve is embedded in the indirect vector controller in per unit form (the quantities that are in per unit in Fig. 12 have an additional index pu). Parameter denoted as SG is a constant (slip gain), equal to $L_{mn}/(T_m \psi_m)$. The inverse magnetizing curve is represented with a simple two-parameter function $i_{m(pu)} = a\psi_{m(pu)} + (1-a)\psi^b_{m(pu)}$, where parameters a and b are the unknowns that need to be determined experimentally. However, it turns out that in the region of the magnetizing flux variation that is of interest (from zero to 1 per unit) the impact of parameter b is small and a convenient value is $b = 7$. In order to determine value of the remaining coefficient a, which impacts significantly on the shape of the inverse magnetizing curve, the machine is operated in the field weakening region under no-load condi-

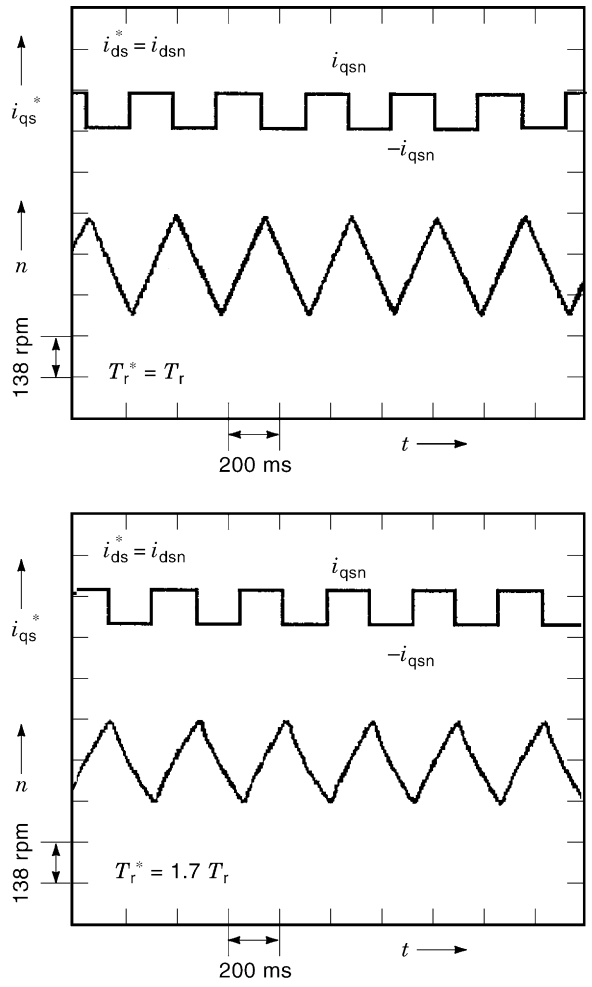

Figure 11. Experimental method of rotor time constant tuning in indirect vector controller: speed response to alternating square-wave torque command with correct rotor time constant and with 1.7 times correct rotor time constant (0.75 kW machine). Speed response is a triangular function of time when rotor time constant is correctly set in the controller. Speed response deviates from triangular when the rotor time constant value is incorrect.

tions, with the base speed set to a convenient value (smaller than in normal operating conditions, but still sufficiently high to make impact of the stator resistance voltage drop on the identification negligible). Fundamental of the line-to-line voltage is measured for various values of the coefficient a at different speeds. Figure 13 illustrates measurement results for $b = 7$ and two values of a, $a = 1$ (saturation neglected) and $a = 0.7$ (saturation over-compensated) for a 4-pole, 50 Hz, 2.3 kW induction machine aimed for servo-drive applications. If the main flux saturation is neglected in the controller ($a = 1$), the stator voltage increases in the field weakening region, so that the voltage margin available for current control reduces. This is one of the reasons why the compensation of magnetizing flux saturation has to be utilized in the field weakening region. In the real drive operation, where field weakening commences above rated speed, there is little voltage left for current control and, unless magnetizing flux saturation is taken care of, voltage margin may completely be lost due to the increase in the machine's back electromotive force. If saturation is over-compensated ($a = 0.7$), the voltage in the field weakening decreases. This means that the stator d-axis current is reduced too much, leading to a decrease in the motor's torque capability. Thus only correct setting of parameters of the inverse magnetising curve enables operation with the correct voltage margin necessary for current control, with torque capability of the motor preserved. Correct setting of the parameters will lead to the practically constant voltage value in the field weakening region, so that, by performing measurements for various values of coefficients a and b, it is possible to determine the most appropriate pair a, b purely by visual inspection of the measured voltage curves. For the machine whose voltage is illustrated in Fig. 13, the correct value of the coefficient a is 0.9.

COMPENSATION OF PARAMETER VARIATION EFFECTS

Sources of parameter changes in an induction machine differ in nature. Stator and rotor resistance variation with temperature is thermal and is inherently slow, as the thermal time constant of the machine is much bigger than the electromagnetic time constants. Parameter variations caused by main flux saturation, leakage flux saturation, and skin effect, as well as the iron loss, are of electromagnetic nature. Change of parameters due to electromagnetic phenomena is much quicker than thermally caused variations, as it is governed by electromagnetic time constants. This principal difference in both the nature of parameter variations and in the rate at which the variations take place has led to the development of two different approaches to compensation of parameter variation effects. Parameter variations due to electromagnetic phenomena are most appropriately compensated if the standard, constant parameter controller is substituted with a modified one that takes into account given parameter variation. This method of compensation is of the open-loop type and it provides compensation in both transient and steady-state operation. Compensation of temperature dependent variation of resistances is most adequately provided by on-line identification of the resistance, which is usually operational in the steady state only.

Compensation of the skin effect related parameter variations in a vector controlled drive can be accomplished by substituting the rotor circuit with two equivalent rotor circuits (16, 33). As there are now two rotor flux space vectors, it is impossible to define a unique rotor flux space vector and the orientation of the stator current space vector is performed with respect to the air-gap flux space vector (16, 33). Rotor leakage flux saturation can be included in the model of the machine by making rotor leakage inductance a variable parameter, dependent on the rotor current (33). Similarly, iron loss representation can be included in the induction machine model, and it is possible to design both an indirect rotor flux oriented controller and the $i_s - \omega$ estimator that fully compensate for the iron loss if such a modified model is used for development of vector control schemes (18, 19). As already noted, all these parameter variation effects are of minor importance when compared to main flux saturation and rotor resistance variation. The

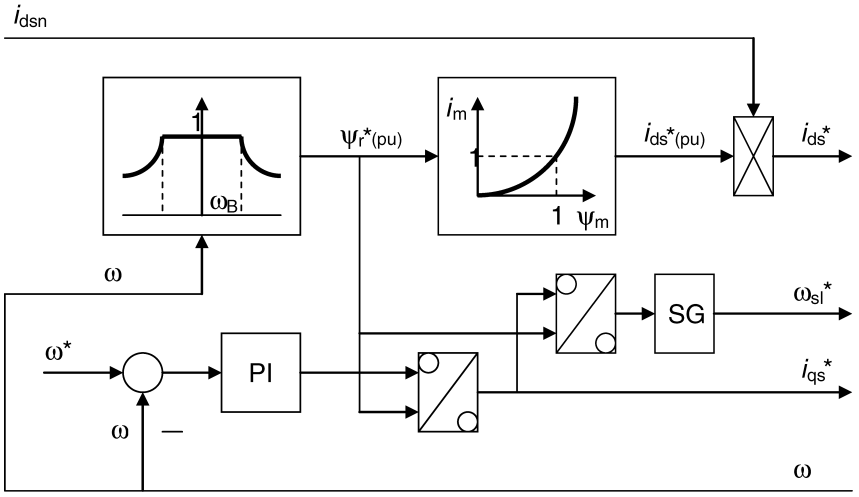

Figure 12. Indirect vector controller with compensation of magnetizing flux saturation for operation in both base speed and field weakening region. Inverse magnetizing curve is embedded in the controller in the form of a conveniently chosen analytical two-parameter function in per unit form. Decrease of the rotor flux reference in the field weakening region is automatically followed by proper stator d-axis current adjustment, since the nonlinearity of the magnetization characteristic is taken into account in the stator d-axis current reference calculation.

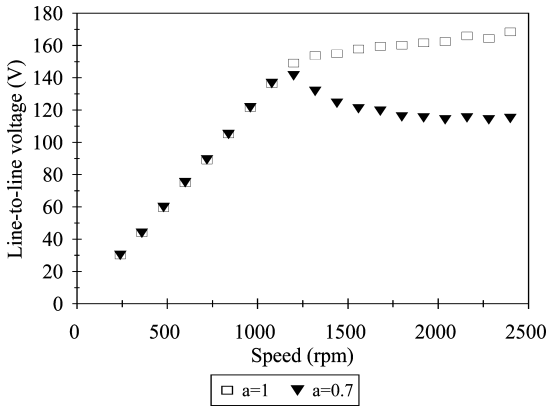

Figure 13. Measured fundamental component of stator line-to-line voltage for $b = 7$ and two values of parameter a. The base speed is set to 1150 rpm and measurements are done in both base speed region and field weakening region. In the base speed region the measurement results coincide since the machine is operated with constant rated rotor flux reference (stator d-axis current). However, in the field weakening region the value of the parameter a significantly impacts on the line-to-line voltage. Neither of the two a values is the correct one.

following discussion therefore concentrates on compensation of the two major sources of detuning.

Compensation of Main Flux Saturation

The approach to main flux saturation compensation, which is to be discussed, is based on modification of the standard d-q-axis model, given by Eqs. (18), (19), and (21) (equivalent T-circuit approach). It is possible to deal with compensation of main flux saturation using other approaches, such as the equivalent π circuit approach (34), or equivalent inverse Γ circuit (equivalent rotor magnetizing current) approach (1, 9), and to develop again appropriate modified vector control schemes.

Equations (18) and (19) are the starting point in derivation of a modified $i_s - \omega$ estimator that fully accounts for main flux saturation. If rotor current space vector is eliminated from Eq. (18), one obtains

$$T_{\sigma r} d\boldsymbol{\psi}_r/dt + j(\omega_a - \omega)\boldsymbol{\psi}_r T_{\sigma r} + \boldsymbol{\psi}_r = \boldsymbol{\psi}_m \tag{38}$$

where rotor leakage time constant is defined as $T_{\sigma r} = L_{\sigma r}/R_r$. Application of the rotor flux orientation constraints, Eqs. (22) and (23), followed by resolution into d-q-axis components, yields the first two equations:

$$\begin{aligned} T_{\sigma r} d\psi_r/dt + \psi_r &= \psi_{dm} \\ \omega_r - \omega = \omega_{sl} &= \psi_{qm}/(T_{\sigma r}\psi_r) \end{aligned} \tag{39}$$

As the dependence of the magnetizing flux on magnetizing current is a known nonlinear function, then from Eq. (8) it follows that the magnetizing current components are

$$\begin{aligned} i_{dm} = \psi_{dm}/L_m &= \frac{\psi_{dm}}{\psi_m} i_m(\psi_m) = i_{dm}(\psi_m) \\ i_{qm} = \psi_{qm}/L_m &= \frac{\psi_{qm}}{\psi_m} i_m(\psi_m) = i_{qm}(\psi_m) \end{aligned} \tag{40}$$

where $i_m = i_m(\psi_m)$ represents inverse magnetizing curve. Application of Eq. (23) in conjunction with Eq. (7) and subsequent substitution of Eq. (40) yields two additional equations of the estimator:

$$\begin{aligned} \psi_{dm} &= \psi_r + L_{\sigma r}[i_{ds} - i_{dm}(\psi_m)] \\ \psi_{qm} &= L_{\sigma r}[i_{qs} - i_{qm}(\psi_m)] \end{aligned} \tag{41}$$

Electromagnetic torque, Eq. (10), can be expressed in rotor flux oriented reference frame as

$$T_e = K\psi_r \psi_{qm}/L_{\sigma r} \tag{42}$$

Equations (39)–(42) describe a saturated current-fed rotor flux oriented induction machine and enable design of a modified rotor flux estimator (Fig. 14) that includes nonlinear function $L_m = f(\psi^2_m)$, obtainable from the no-load mag-

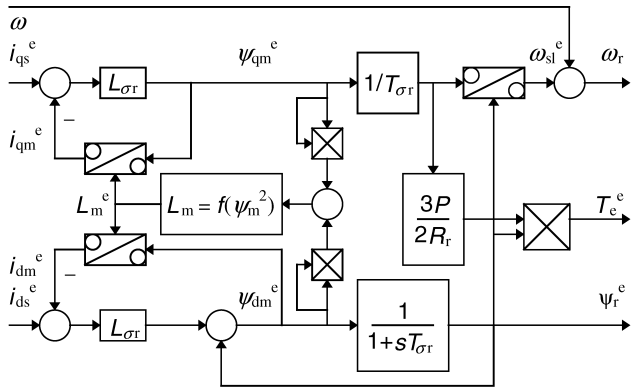

Figure 14. A modified rotor flux estimator with compensation of main flux saturation. The estimator recognizes changes in saturation level due to both variation of the rotor flux reference and cross saturation and thus provides instantaneous adaptation to the actual saturation level in the machine.

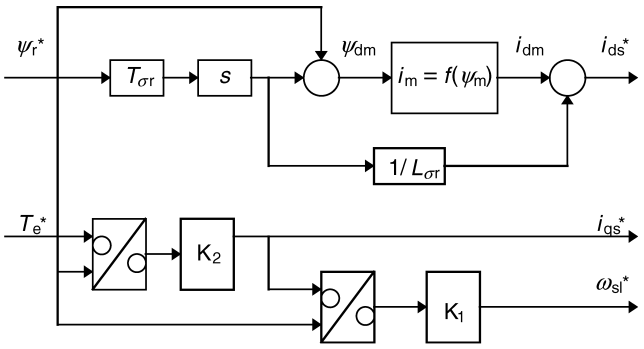

Figure 15. A modified indirect rotor flux oriented controller with partial compensation of main flux saturation. The controller compensates for change in saturation level due to change in rotor flux reference and ignores the cross-saturation effect. By setting $sT_{\sigma r}\psi_r^* \approx 0$ the controller reduces to the form already shown in Fig. 12.

netizing curve. The modified estimator compensates for a change of saturation level due to both change in reference flux setting and due to the cross-saturation effect. Operation of the scheme of Fig. 2, when the estimator of Fig. 14 is used, is examined in Ref. 26 for the same reversing transient already discussed in conjunction with Fig. 8. The estimator of Fig. 14 correctly detects a tendency of the rotor flux to decrease during the reversal. As a consequence, the PI flux controller increases the reference stator d-axis current, and the rotor flux in the machine remains at almost constant value. Estimated torque and actual torque are in good agreement as well. Similarly, if a change in the saturation level in the machine takes place due to variation of the stator current d-axis command, the estimator correctly detects this change and again provides full compensation (26).

Modified indirect vector controller can be designed by utilizing Eqs. (39)–(42) as the starting point. However, if one recalls that the main reason for widespread application of the indirect rotor flux oriented control is its simplicity, then it is desirable to minimize the increase in complexity due to addition of main flux saturation compensation. A possibility is to provide only partial compensation, by ignoring two phenomena (35). First, the impact of cross-saturation is pronounced only if the machine operates with very high transient torques. If this is not the case, the q-axis component of the magnetizing flux is small and its contribution to the total magnetizing flux can be neglected. Second, calculation of reference stator q-axis current reference and calculation of the reference angular frequency in Eqs. (29) and (30) involve the ratio of magnetizing to rotor inductance. Change in this ratio is always small and may be neglected. These two approximations enable development of the controller equations separately for the d-axis and q-axis. From Eqs. (39) and (41), taking the first approximation into account, one gets

$$\begin{aligned} \psi_m &\approx \psi_{dm} = T_{\sigma r} d\psi_r^*/dt + \psi_r^* \\ i_{ds}^* &= i_{dm}(\psi_m) + (1/L_{\sigma r}) T_{\sigma r}\, d\psi_r^*/dt \end{aligned} \tag{43}$$

while equations for stator q-axis current command and for the angular slip frequency command of Eqs. (29) and (30) remain unchanged:

$$\begin{aligned} \omega_{sl}^* &= K_1 i_{qs}^*/\psi_r^* \qquad K_1 = R_r L_{mn}/(L_{\sigma r} + L_{mn}) \\ i_{qs}^* &= K_2 T_e^*/\psi_r^* \qquad K_2 = (1/K)(L_{\sigma r} + L_{mn})/L_{mn} \end{aligned} \tag{44}$$

Figure 15 shows indirect rotor flux oriented controller with partial compensation of main flux saturation (35). It provides compensation when the machine operates with variable d-axis current command. If rate of change of rotor flux is neglected, the form of this modified indirect vector controller reduces to the one already illustrated in Fig. 12 (except that per unit representation is used in Fig. 12 and speed control loop is included).

Compensation of Rotor Resistance Variation

Rotor resistance plays a crucial role in establishing the accurate rotor flux oriented control in both schemes considered here, and most of the research in the area of compensation of parameter variation effects has been devoted to rotor resistance tuning. A number of various methods are available (30, 36). Due to the thermal nature of rotor resistance variation, compensation consists of on-line rotor resistance identification. The prevailing method is based on principles of model reference adaptive control and is dominant due to its relatively simple implementation. The idea is that one quantity can be calculated in two different ways. The first value is calculated from references inside the control system. The second value is calculated from measured signals. The difference between the two is an error signal, whose existence is assigned entirely to the error in rotor resistance. The error signal drives an adaptive mechanism (PI or I controller) that provides correction of the rotor resistance. Many methods belong to this group (37–41) and they primarily differ with respect to which quantity is selected for adaptation purposes. The reactive power method does not involve stator resistance and is therefore frequently applied (37, 38). Other possibilities include methods based on the special criterion function (39), air-gap power (40), torque (38, 41), rotor flux magnitude (38), stator voltage d- or q-axis components (38), etc. There are a couple of common features that all these methods share. First, rotor resistance adaptation is usually opera-

tional in steady states only and is therefore based on the steady-state model of the machine. Second, stator voltages are usually required for calculation of the adaptive quantity and they have to be either measured or reconstructed from the inverter firing signals and measured dc link voltage (11). Third, identification usually does not work at zero speed and at zero load torque. Finally, identification relies on the model of the machine, in which, most frequently, all the other parameters are treated as constants. This is at the same time the major shortcoming of this group of methods. An analysis of the parameter variation influence on accuracy of rotor resistance adaptation (42) shows that, if other parameters vary, performance of the drive with resistance identifier can be worse than performance without the identifier. The other drawback, impossibility of adaptation at zero speed and zero load torque, is sometimes successfully eliminated (39).

The principle of model reference adaptive control approach is elaborated next, using reactive power as the reference and adaptive quantity. Rotor resistance adaptation utilizes a steady-state model of the machine. The input reactive power is given in terms of d-q-axis quantities by

$$Q_e = (3/2)(v_{qs}i_{ds} - v_{ds}i_{qs}) \tag{45}$$

Stator voltage equations in rotor flux oriented reference frame are in the steady state (9):

$$\begin{aligned} v_{ds} &= R_s i_{ds} - \omega_r \sigma L_s i_{qs} \\ v_{qs} &= R_s i_{qs} + \omega_r \sigma L_s i_{ds} + \omega_r (L_m/L_r)\psi_r \end{aligned} \tag{46}$$

where $\sigma = 1 - L^2_m/L_s L_r$. In steady-state operation with correct rotor flux orientation, $\psi_r = L_m i_{ds}$. If this condition is taken into account and Eq. (46) is substituted into Eq. (45), the following correlation is obtained:

$$v_{qs}i_{ds} - v_{ds}i_{qs} = \omega_r L_s i^2_{ds} + \omega_r \sigma L_s i^2_{qs} \tag{47}$$

The rotor resistance adaptation mechanism is constructed using Eq. (47). The reference quantity is defined in terms of reference stator d-q-axis currents using the right-hand side of Eq. (47), while the estimated value of the same quantity is calculated on the basis of the measured stator voltages and currents, using the left-hand side of Eq. (47). As power is invariant with respect to the reference frame, the left-hand side is calculated using voltages and currents in the stationary reference frame. Thus finally

$$\begin{aligned} Q^*_e &= (3/2)(\omega_r L_s i^{*2}_{ds} + \omega_r \sigma L_s i^{*2}_{qs}) \\ Q^e_e &= (3/2)(v_{\beta s}i_{\alpha s} - v_{\alpha s}i_{\beta s}) \end{aligned} \tag{48}$$

The adaptation mechanism is independent of the stator resistance, which is a good feature of this method. All the inductances are assumed to be constant. The difference between the two reactive powers of Eq. (48) is assigned to discrepancies between rotor resistance value used in the controller and the actual one. This error signal is processed through a PI controller, whose output is an updated rotor resistance value, which is subsequently used in calculation of the reference slip command. Figure 16 illustrates the adaptation mechanism, where operation in the constant rotor flux region is assumed and the output of the corrective PI controller is shown as the inverse of the rotor time constant.

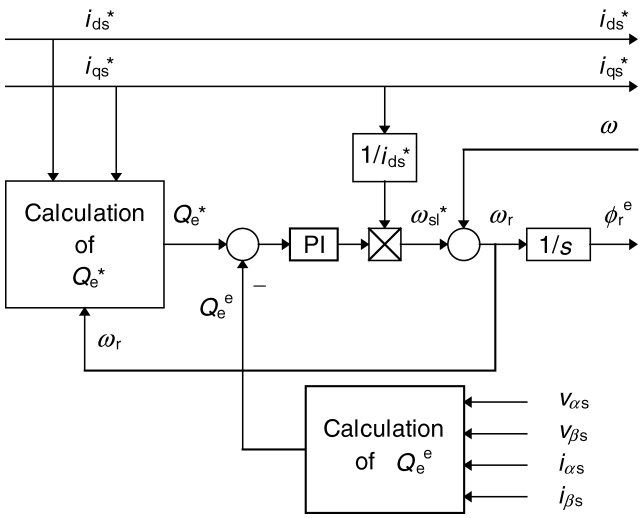

Figure 16. Rotor resistance on-line adaptation mechanism using approach based on model reference adaptive control. The difference between the two reactive powers is an error signal used to drive a PI controller, whose output is shown here as inverse of the rotor time constant.

The reactive power method is sensitive to inductance variation. A convenient way of eliminating this drawback is to combine vector control schemes that include compensation of main flux saturation (Figs. 14 or 15) with the rotor resistance identifier of Fig. 16. Information on magnetizing inductance is then passed from the modified indirect vector controller (or rotor flux estimator) to the resistance identifier, while the resistance identifier supplies the indirect controller (or flux estimator) with updated values of the rotor resistance. It is thus possible to compensate for both effects by combining the two methods of parameter variation compensation (39). Figure 17 illustrates operation of such a rotor resistance adaptation scheme by means of experimentally recorded traces. The error function, which serves as the input to the PI controller, is shown together with the rotor resistance estimate in per unit (i.e., ratio of rotor resistance in the controller to the actual one in the machine). The drive operates at zero speed with 0.2 per unit load torque. The adaptation mechanism operation is illustrated for step variation of rotor resistance used in the controller of ±50%. The adaptation mechanism always returns rotor resistance in the controller to the previous value (i.e., to $R^*_r/R_r = 1$).

OPTIMAL EFFICIENCY CONTROL

Since the torque of an induction motor drive is a product of two adjustable variables, namely, the flux amplitude and the active component of the stator current, the existing degree of freedom provides the means for reducing the power conversion losses through the flux level adjustment. By varying the flux amplitude (i.e. rotor flux reference), a better balance between iron and copper losses can be achieved as a function of the actual motor loading, thus improving the drive efficiency. The vector controlled drives with the

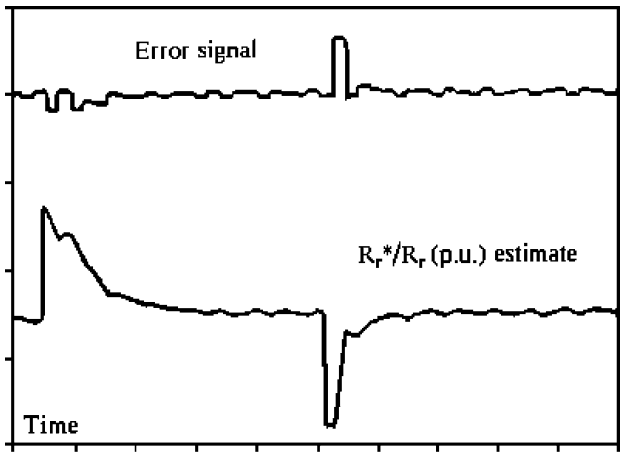

Figure 17. Experimentally recorded operation of the rotor resistance adaptation in an indirect rotor flux oriented induction machine. Rotor resistance in the controller is deliberately detuned by ±50% in a stepwise manner. The rotor resistance identifier always returns the value to the correct one. (Scales: time—10 s/div, error function—0.5 p.u./div, rotor resistance estimate—0.4 p.u./div; 0.75 kW machine.) Figure provided courtesy of Dr. S. N. Vukosavic, Department of Electrical Engineering, University of Belgrade, Belgrade, Yugoslavia.

greatest potential for energy saving are the drives operating in the constant torque mode with frequent light load intervals. A typical example is the elevator drives (43), which run mostly with less than a half of the rated torque. Power loss reduction in an induction motor drive is most easily achieved by implementing a loss minimisation controller, usually called optimal efficiency controller. An extensive overview of the existing approaches to optimal efficiency control is provided in (44), where two distinct groups of methods, applicable in conjunction with vector controlled drives, have been identified: i) a loss model based controller (LMC) and ii) a search controller (SC).

The search controllers (SC) (23, 45, 46) require measurement of the drive's input power and they minimise the input power by iterative adjustments of the flux reference. Input power is a parabolic function of the flux, that has strictly positive second derivative with the regime-dependent minimum that can be found by various search procedures (23, 45), including fuzzy and neuro-fuzzy methods (46, 47). The SC solutions have unprecedented parameter independence and the precision is compromised only when the input power dependence on flux is too smooth and flat around the minimum. However, even with a constant output power, a SC never reaches the steady state and produces continuous flux and torque pulsations around the optimum operating point. Due to the search nature of the algorithm the adjustment of the flux reference to the optimal value for any particular load takes a considerable time. With search times of well over a second duration and even exceeding seven seconds, the SC is of no practical value in drives with fast changing loads. Hence, the problem of slow convergence is the major drawback of SCs.

In contrast to the SC approach, response of the LMCs is smooth and fast, for they use a functional model of the system losses to determine the optimum flux reference for the given load and speed. This is the main advantage of the LMC approach over the SC method and is a logical solution for all the contemporary drives, which have *d-q* reference frame based control system and therefore anyway require some knowledge regarding the controlled motor. Regardless of how a loss model controller is applied, accurate values of motor parameters are required for the correct operation (48, 49). The algorithm must include iron losses, since optimal efficiency operation can only be obtained by proper balancing of iron and copper losses for any particular load/speed. Further, since the idea is to operate with a variable rotor flux reference setting, magnetizing flux saturation representation has to be included in the model as well. These are the major drawbacks of the LMC approach to optimal efficiency control. In practice, successful LMC applications (43, 49, 50–53) deal with a simplified loss function considering the main flux-dependent power losses, while neglecting the secondary loss components. LMC approach is therefore heavily dependent on parameter variation effects and simplifying assumptions made in the formulation of the loss function. These LMC drawbacks lead to a sub-optimal flux setting.

In summary, none of the two mainstream approaches to optimal efficiency control is ideal. Search algorithms are inherently independent of the machine's parameters and hence parameter variation effects as well, but are slow in providing convergence of the rotor flux reference setting to the optimal value. On the other hand, model based controllers are inherently fast but are heavily dependent on the accuracy of the model used to represent the machine's losses in the control algorithm, leading often to suboptimal flux reference setting. To overcome the shortcomings of both methods, while simultaneously keeping their advantages, it is possible to implement an on-line identification routine for the loss function parameters (54). The algorithm (54) can therefore be viewed as combining good features of both the search controllers and loss model controllers, while simultaneously eliminating the major shortcomings of these two methods. The need for precise knowledge of the motor loss function parameters, which is the major drawback of the LMC (while lack of it is the main advantage of the SC) is eliminated by the on-line identification routine. On the other hand, the problem of slow convergence towards optimum efficiency point, which is the main drawback of the SC (while fast convergence is the major advantage of the LMC) does not occur since the algorithm operates in a similar way to ordinary LMCs.

An experimentally obtained illustration of the operation of the optimal efficiency controller is shown in Fig. 18 for a 4-pole, 50 Hz, 2.2 kW induction motor drive. Variations of the drive's input power and flux are depicted for two types of optimal efficiency control: application of a search controller and utilization of the controller with on-line loss function identification (On-LineLFI) of (54). The machine operates at 1450 rpm and the load torque is pulsed from 1 to 15 Nm, at first with a 10 second period and then with a 4 second period. When load torque varies relatively slowly (10 s period) the SC manages to establish optimal efficiency operating point for each load torque value, as evidenced by the flux reaching the steady state before the subsequent load torque change. The steady state flux and input power

values obtained with On-LineLFI based controller and the SC are equal for both high and low load torque values. However, the SC waveforms are slow on the load transients. For the load cycle shown in the upper part of Fig. 18, On-LineLFI based controller reduces the overall energy consumption by 13.32%, compared to the SC. The situation changes if the load torque varies rapidly, as shown in the bottom part of Fig. 18, where load torque period is only 4 seconds. The SC controller now does not manage to establish the operation with the optimum flux adjustment, due to its slow convergence and rapid nature of the load torque change. In contrast to that, the On-LineLFI controller is characterised with extremely rapid convergence, so that the optimum flux level is reached during the drive operation for each torque value setting without any difficulty. In this case the On-LineLFI controller reduces the power consumption by 26.5 %, compared to the SC controller.

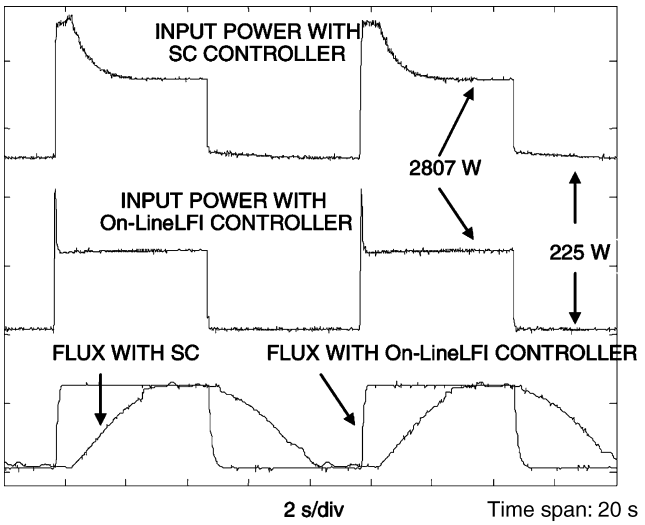

Figure 18. Experimentally recorded traces of the flux and input power: comparison of the performance of the On-LineLFI controller and the search controller. The machine runs at 1450 rpm and the load torque steps from approximately 1 Nm to 15 Nm and back. The drive is running in the speed control mode, and the load pulsing is performed by switching the resistive load in the armature circuit of the DC machine. The period of load torque variation is 10 seconds in the upper part and 4 seconds in the lower part of the figure. Response of SC is much slower and, for rapidly varying load torque (bottom part), the SC does not manage to establish operation with optimum efficiency before the load torque changes again.

SPEED-SENSORLESS CONTROL

It has been assumed throughout this article so far that a vector controlled induction machine is equipped with a speed or position sensor. Speed/position sensor is the weak point of the drive as it considerably increases cost, requires space for mounting and has to be electrically connected to the controller. This leads to reduction in reliability of the drive with an increase in cost and it is highly desirable to eliminate the speed (position) sensor. Such a situation has initiated development of numerous so-called speed-sensorless vector controlled induction motor drives, that rely on speed estimation rather than on speed (position) measurement. Approaches to speed estimation vary to the great extent but are almost exclusively based on measurement of either stator currents only, or stator currents and stator voltages (5,9,11,55,56). In general, two major approaches can be identified. The first one encompasses the techniques that estimate rotor speed from the stator current spectrum, while the second one relies on utilisation of an induction machine model and the speed estimator is either of open-loop or closed-loop type (55, 56). Model-based approaches are in general easy to implement and good performance can be obtained in the medium to high speed region without much difficulty. However, model-based approach cannot provide reliable speed estimation at very low stator frequencies and the major effort has been directed in recent times towards overcoming the problems encountered in speed estimation around zero speed. For this purpose spectrum based speed estimation methods are applied.

One of the problems with model based speed estimation techniques is the sensitivity to induction motor parameter variation effects. Since the speed estimation utilizes an induction motor model, the accuracy of the speed estimate is heavily dependent on the accuracy of the motor parameters used in the calculations. In addition to the already considered parameter variation affects (rotor resistance variation and main flux saturation), model-based speed estimation is typically also sensitive to stator resistance variation. As a matter of fact, the accuracy of this parameter is of utmost importance for accurate speed estimation at low stator frequencies where stator resistance voltage drop represents a significant portion of the total applied voltage.

The majority of the model-based closed-loop speed estimators are in essence of structures practically identical to those discussed in the section on compensation of rotor resistance variation. In speed-sensored drives speed is known (since it is measured) and rotor resistance is adapted on-line. In speed-sensorless drives rotor resistance is regarded as known and speed is estimated instead.

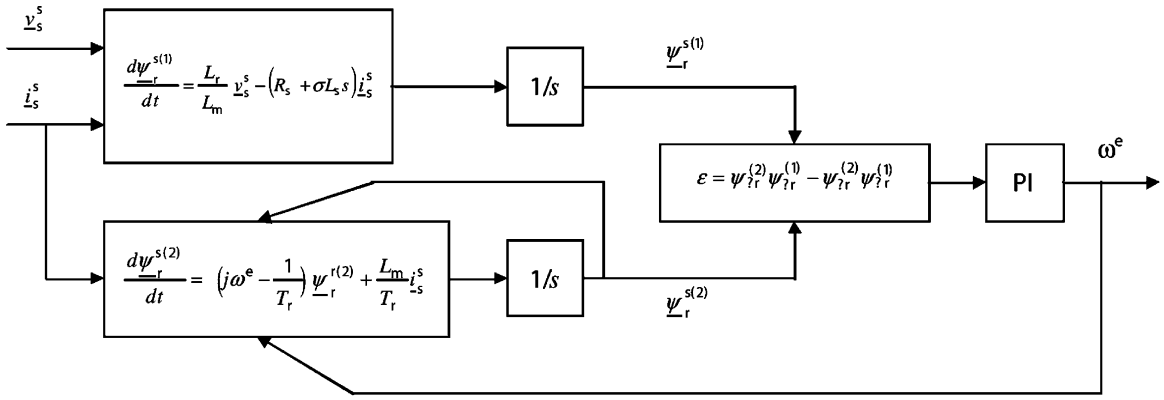

Figure 19. Basic structure of the model reference adaptive control type of speed estimator: rotor flux space vector is estimated using two different models and the angular position of the adaptive estimate is forced to track the one of the reference model, using an error quantity that is processed by a PI controller.

One procedure often used to estimate the speed in speed-sensorless drives is model reference adaptive control approach, of the type illustrated in Fig. 16 in conjunction with rotor resistance on-line identification. While it is possible to utilize reactive power again, a more frequent choice is in this case rotor flux space vector (57). Stator voltages have to be measured (or reconstructed), together with stator currents. The speed estimator operates in the stationary reference frame and the rotor flux space vector is expressed from two Equations (18), using Eqns. (19), in two different ways:

$$\frac{d\psi_{\mathrm{r}}^{\mathrm{s}(1)}}{dt} = \frac{L_{\mathrm{r}}}{L_{\mathrm{m}}}[\underline{\mathrm{v}}_{\mathrm{s}}^{\mathrm{s}} - (R_{\mathrm{s}} + \sigma L_{\mathrm{s}} s)\underline{\mathrm{i}}_{\mathrm{s}}^{\mathrm{s}}] \tag{49}$$

$$\frac{d\psi_{\mathrm{r}}^{\mathrm{s}(2)}}{dt} = (\, j\omega^{\mathrm{e}} - \frac{1}{T_{\mathrm{r}}})\psi_{\mathrm{r}}^{\mathrm{r}(2)} + \frac{L_{\mathrm{m}}}{T_{\mathrm{r}}}\underline{\mathrm{i}}_{\mathrm{s}}^{\mathrm{s}} \tag{50}$$

All the machine parameters in Equations (49)–(50) are taken as constant values that correspond to the rated operating conditions. Coefficient σ is once more the total leakage coefficient of the machine, $\sigma = 1 - L_{\mathrm{m}}^2/(L_{\mathrm{s}}L_{\mathrm{r}})$. The rotor flux estimate of Eq. (49) is independent of the rotor speed and it therefore represents the output of the reference model. The second rotor flux estimate (output of Eq. (50)) depends on the estimated speed and it is forced to follow the first estimate by adaptively adjusting the estimated speed. For that purpose an error quantity is defined,

$$\varepsilon = \psi_{\alpha\mathrm{r}}^{(2)}\psi_{\beta\mathrm{r}}^{(1)} - \psi_{\beta\mathrm{r}}^{(2)}\psi_{\alpha\mathrm{r}}^{(1)}$$

and this error quantity is forced to zero using a PI controller, as shown in Fig. 19. As is evident from Eq. (51) and Fig. 19, the adaptive mechanism relies on the error quantity that represents the difference between the instantaneous angular positions of the two rotor flux estimates.

Basic structure of the speed estimator, as illustrated in Fig. 19, suffers from two major shortcomings. The fist one is the pure integration in the reference model, which cannot be utilized in real-world applications since any offset in measurements gets replicated at the integrator output as a quantity that linearly increases in time towards infinity. Hence the pure integration in Eq. (49) and Fig. 19 has to be replaced with either filters (57) or with more sophisticated integrating algorithms (58). The other problem is associated with inaccuracies in the stator resistance value, used in the reference model, at low supply frequencies. Successful operation of this estimator at low but non-zero frequencies is only possible if an appropriate on-line stator resistance estimation algorithm is employed. The possibilities are numerous (30), but one exceptionally well suited approach to on-line stator resistance adaptation is utilisation of the remaining degree of freedom within the speed estimator for that purpose. As noted, speed estimation utilises the angular error in the position of the two rotor flux space vectors. The remaining degree of freedom, difference in the rotor flux magnitudes, can be utilized for stator resistance adaptation (59). This leads to a parallel speed estimator/stator resistance identification scheme that enables stable drive operation for short periods of time even at zero speed under the most difficult (no-load) conditions (59).

Operation of the speed estimator of Fig. 19, where pure integration in the reference model is replaced with a modified integrating algorithm of (58), is illustrated in Fig. 20 for a 2.3 kW, 4-pole, 50 Hz induction motor drive. Traces of estimated and actual speed are shown for two acceleration transients. In the first case the machine is under no-load conditions and reference speed is stepped from zero to 900 rpm, while in the second case the speed is stepped to 1500 rpm and the machine is loaded with a dc generator. As can be seen from Fig. 20, the actual speed traces (obtained by means of a resolver) and the estimated speed traces practically coincide.

Introduction of the modified integration algorithm and stator resistance on-line identification enable successful application of the speed estimator at all speeds from very low ones up to the rated. However, successful utilisation of this speed estimator (and all the other model based estimators) in the field weakening region requires modification of the structure, when compared to Equations (49)–(50). This is so since, once more, the effect of de-saturation in the magnetizing flux (i.e. increase in the magnetizing inductance) has to be compensated. The modified, saturation adaptive, structure of the rotor flux based speed estimator requires

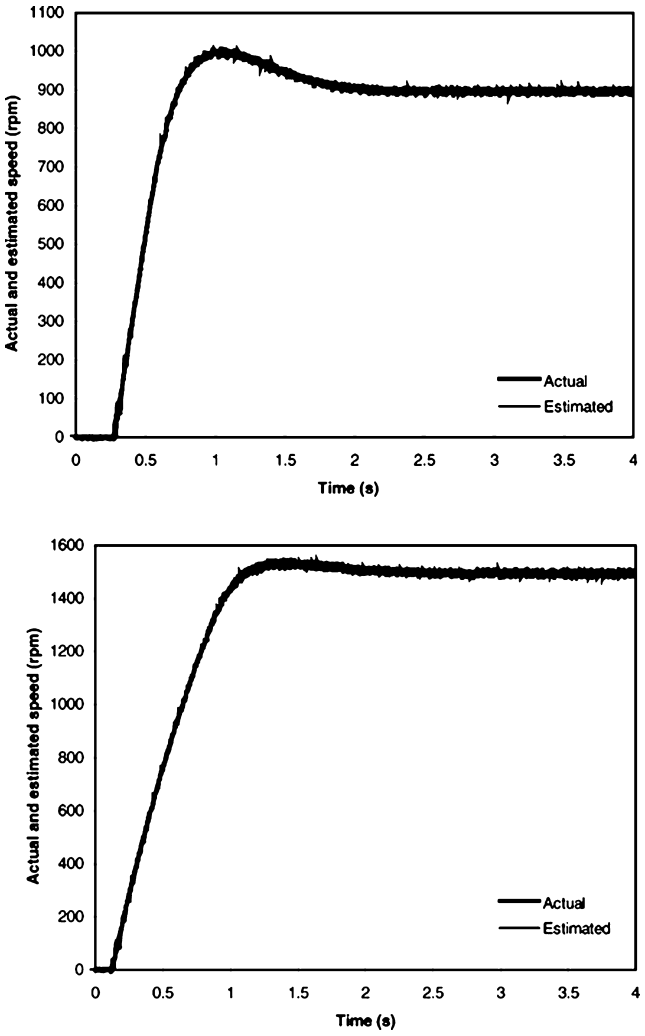

Figure 20. Comparison of the actual (measured) speed and speed estimate obtained using the model based scheme of Fig. 19 for two transients: in the first case speed reference is stepped to 900 rpm and the machine is unloaded (top), while in the second case the speed reference is stepped to 1500 rpm and the machine is loaded using a dc generator. The difference between the estimated speed and the actual speed is negligibly small, as the traces are fully overlapped across the entire transient duration.

modification of the reference model, so that the magnetizing inductance estimation is incorporated and conducted prior to the rotor flux space vector calculation (60). Magnetizing inductance estimate is then utilized in calculation of the rotor flux in both reference model and the adjustable model. It is interesting to note that the structure of the adjustable model remains as in Eq. (50) but the magnetizing inductance value is now a parameter that is continuously adjusted on-line, using the identified value that corresponds to the given speed reference (i.e. rotor flux reference). Comparison of the estimated speed and the actual speed for operation in the field weakening region with reference speed set to just over twice the base speed and applied in a step-wise manner (so that the rotor flux reference is just below 50% of the rated value in final steady state) is shown in Fig. 21. Tracking is excellent and the

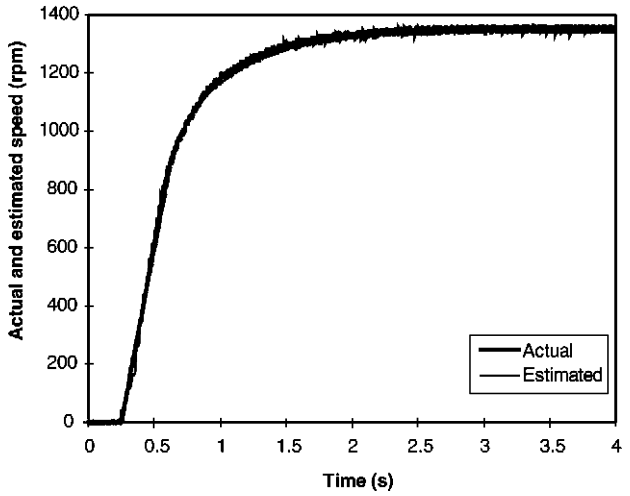

Figure 21. Illustration of the quality of operation of a modified rotor flux based speed estimator, where variation in the main flux saturation in the field weakening is compensated: actual speed and estimated speed in no-load acceleration transient, for speed reference 1350 rpm and the base speed set to 650 rpm.

speed estimation error that would have been present had the magnetizing inductance been held at the rated value in the estimator is fully eliminated.

TRENDS IN VECTOR CONTROL OF INDUCTION MACHINES

The problem of parameter variations is nowadays well understood and many solutions are available. This statement applies to both speed-sensored and speed-sensorless model based vector control schemes. A number of more complicated but simultaneously more accurate (i.e. less sensitive to parameter variation effects) approaches to rotor flux and/or speed estimation, not discussed in any detail here, have been developed over the years. For example, one possibility of improving the accuracy of rotor flux position estimation consists in use of observers (5,56,61) or extended Kalman filters (56, 62). Rotor flux estimation can in both cases be combined with on-line parameter identification (11, 63, 64). A detailed treatment of various observer based and extended Kalman filter based approaches to vector control scheme formulation is available in (56).

Vector control of induction machines has been in the focus of research interest in the last three decades of the twentieth century and, as far as speed-sensored drives are concerned, it is difficult to foresee any substantial new developments in the future. The problem of speed estimation at very low and zero speeds, relevant for speed-sensorless vector controlled drives, is still a topic under significant scrutiny. Nevertheless, only minor improvements over the already available solutions are likely.

In recent times the emphasis has shifted from vector control of three-phase machines to vector control of multiphase (i.e. machines with more than three phases) machines. This has predominantly resulted from developments in three very specific application areas, namely electric ship propulsion, traction (including electric and

hybrid electric vehicles) and the concept of 'more-electric' aircraft. While the specific reasons for looking at a multiphase motor drive utilization in these application areas vary to a large extent (as does the specific ac motor type and the power electronic converter topology), the common feature is that utilisation of multiphase motor drives is perceived as offering important advantages when compared to the use of their three-phase counterparts. As far as multiphase induction machines are concerned, they are predominantly considered for high power applications (electric ship propulsion, locomotive traction and similar) and low voltage, high current applications (electric and hybrid electric vehicles, for example). Utilization of more than three phases brings in this case two main advantages: i) total drive power is split over a larger number of phases, so that the required converter switch rating is lower, compared to an equivalent three-phase drive; ii) using more than three phases improves fault tolerance, since multiphase motor drives can continue to operate with a rotating field after loss of one (or more, depending on the phase number) phases, in contrast to three-phase machines. From the point of view of vector control, basic principles, basic control schemes, and basic problems associated with parameter variation effects, are the same as in three-phase vector controlled induction motor drives. However, utilisation of more than three phases, while being advantageous for the above given reasons, also leads to some new problems that do not exist in three-phase induction motor drives. These are predominantly associated with the quality of the supply provided to the machine, which normally comes from voltage source inverters. Although considerable developments in this area have taken place during the last decade, exciting new achievements may be expected.

BIBLIOGRAPHY

1. D. W. Novotny and T. A. Lipo, *Vector Control and Dynamics of AC Drives*, Oxford: Clarendon Press, 1996.
2. F. Blaschke, Das Prinzip der Feldorientierung, die Grundlage für die TRANSVECTOR—Regelung von Drehfeldmaschinen, *Siemens—Zeitschrift*, **45**: 757–760, 1971.
3. I. Boldea and S. A. Nasar, *Vector Control of AC Drives*, Boca Raton, FL: CRC Press, 1992.
4. P. Vas, *Vector Control of AC Machines*, Oxford: Clarendon Press, 1990.
5. A. M. Trzynadlowski, *The Field Orientation Principle in Control of Induction Motors*, Norwell, MA: Kluwer Academic Publishers, 1994.
6. P. C. Krause, O. Wasynczuk, and S. D. Sudhoff, *Analysis of Electric Machinery*, Piscataway, NJ: IEEE Press, 1995.
7. P. Vas, *Electric Machines and Drives—A Space Vector Theory Approach*, Oxford: Clarendon Press, 1992.
8. A. Hughes, J. Corda, and D. A. Andrade, Vector control of cage induction motors: a physical insight, *IEE Proc. Electr. Power Appl.*, **143**: 59–68, 1996.
9. W. Leonhard, *Control of Electrical Drives*, 2nd ed., Berlin: Springer-Verlag, 1996.
10. X. Xu and D. W. Novotny, Selection of the flux reference for induction machine drives in the field weakening region, *IEEE Trans. Ind. Appl.*, **28**: 1353–1358, 1992.
11. P. Vas, *Parameter Estimation, Condition Monitoring, and Diagnosis of Electrical Machines*, Oxford: Clarendon Press, 1993.
12. R. Joetten and G. Maeder, Control methods for good dynamic performance induction motor drives based on current and voltage as measured quantities, *IEEE Trans. Ind. Appl.*, **IA-19**: 356–363, 1983.
13. E. Y. Ho and P. C. Sen, Decoupling control of induction motor drives, *IEEE Trans. Ind. Electron.*, **35**: 253–262, 1988.
14. R. W. De Doncker and D. W. Novotny, The universal field oriented controller, *IEEE Trans. Ind. Appl.*, **30**: 92–100, 1994.
15. R. W. De Doncker, F. Profumo, M. Pastorelli and P. Ferraris, Comparison of universal field oriented (UFO) controllers in different reference frames, *IEEE Trans. Power Electron.*, **10**: 205–213, 1995.
16. R. W. De Doncker, Field-oriented controllers with rotor deep bar compensation circuits, *IEEE Trans. Ind. Appl.*, **28**: 1062–1071, 1992.
17. R. W. De Doncker, Parameter sensitivity of indirect universal field-oriented controllers, *IEEE Trans. Power Electron.*, **9**: 367–376, 1994.
18. E. Levi, Impact of iron loss on behaviour of vector controlled induction machines, *IEEE Trans. Ind. Appl.*, **31**: 1287–1296, 1995.
19. E. Levi, M. Sokola, A. Boglietti and M. Pastorelli, Iron loss in rotor flux oriented induction machines: identification, assessment of detuning and compensation, *IEEE Trans. Power Electron.*, **11**: 698–709, 1996.
20. I. T. Wallace, D. W. Novotny, R. D. Lorenz and D. M. Divan, Verification of enhanced dynamic torque per ampere capability in saturated induction machines, *IEEE Trans. Ind. Appl.*, **30**: 1193–1201, 1994.
21. R. D. Lorenz and D. W. Novotny, Saturation effects in field-oriented induction machines, *IEEE Trans. Ind. Appl.*, **26**: 283–289, 1990.
22. H. Grotstollen and J. Wiesing, Torque capability and control of a saturated induction motor over a wide range of flux weakening, *IEEE Trans. Ind. Electron.*, **42**: 374–381, 1995.
23. D. S. Kirschen, D. W. Novotny and T. A. Lipo, On-line efficiency optimization of a variable frequency induction motor drive, *IEEE Trans. Ind. Appl.*, **IA-21**: 610–616, 1985.
24. E. Levi, A unified approach to main flux saturation modelling in d-q axis models of induction machines, *IEEE Trans. Energy Convers.*, **10**: 455–461, 1995.
25. E. Levi and V. Vuckovic, Field-oriented control of induction machines in the presence of magnetic saturation, *Electric Machines and Power Systems*, **16**: 133–147, 1989.
26. E. Levi, Magnetic saturation in rotor flux oriented induction motor drives: operating regimes, consequences and open-loop compensation, *European Transactions on Electrical Power Engineering*, **4**: 277–286, 1994.
27. R. Krishnan and F. C. Doran, Study of parameter sensitivity in high-performance inverter-fed induction motor drive systems, *IEEE Trans. Ind. Appl.*, **IA-23**: 623–635, 1987.
28. K. B. Nordin, D. W. Novotny and D. S. Zinger, The influence of motor parameter deviations in feedforward field orientation drive systems, *IEEE Trans. Ind. Appl.*, **IA-21**: 1009–1015, 1985.
29. O. Ojo, M. Vipin and I. Bhat, Steady-state performance evaluation of saturated field-oriented induction machines, *IEEE Trans. Ind. Appl.*, **30**: 1638–1647, 1994.

30. H. A. Toliyat, E. Levi, and M. Raina, A review of RFO induction motor parameter estimation techniques, *IEEE Trans. Energy Convers.*, **18**: 271–283, 2003.
31. E. Levi, M. Sokola, and S. N. Vukosavic, A method of magnetising curve identification in rotor flux oriented induction machines, *IEEE Trans. Energy Convers.*, **15**: 157–162, 2000.
32. R. D. Lorenz, Tuning of field oriented induction motor controllers for high performance applications, *Proc. Annu. Meet. IEEE Ind. Appl. Soc.*, **20**: 607–612, 1985.
33. S. Williamson and R. C. Healey, Space vector representation of advanced motor models for vector controlled induction motors, *IEE Proc. Electr. Power Appl.*, **143**: 69–77, 1996.
34. C. R. Sullivan, C. Kao, B. M. Acker and S. R. Sanders, Control systems for induction machines with magnetic saturation, *IEEE Trans. Ind. Electron.*, **43**: 142–152, 1996.
35. E. Levi, S. Vukosavic and V. Vuckovic, Saturation compensation schemes for vector controlled induction motor drives, *Proc. Annu. IEEE Power Electron. Spec. Conf.*, **21**: 591–598, 1990.
36. R. Krishnan and A. S. Bharadwaj, A review of parameter sensitivity and adaptation in indirect vector controlled induction motor drive systems, *IEEE Trans. Power Electron.*, **6**: 695–703, 1991.
37. L. J. Garces, Parameter adaption for the speed-controlled static ac drive with a squirrel-cage induction motor, *IEEE Trans. Ind. Appl.*, **IA-16**: 173–178, 1980.
38. T. M. Rowan, R. J. Kerkman and D. Leggate, A simple on-line adaption for indirect field orientation of an induction machine, *IEEE Trans. Ind. Appl.*, **27**: 720–727, 1991.
39. S. N. Vukosavic and M. R. Stojic, On-line tuning of the rotor time constant for vector-controlled induction motor in position control applications, *IEEE Trans. Ind. Electron.*, **40**: 130–138, 1993.
40. D. Dalal and R. Krishnan, Parameter compensation of indirect vector controlled induction motor drive using estimated airgap power, *Proc. Annu. Meet. IEEE Ind. Appl. Soc.*, **22**: 170–176, 1987.
41. R. D. Lorenz and D. B. Lawson, A simplified approach to continuous, on-line tuning of field-oriented induction machine drives, *IEEE Trans. Ind. Appl.*, **26**: 420–424, 1990.
42. A. Dittrich, Parameter sensitivity of procedures for on-line adaptation of the rotor time constant of induction machines with field oriented control, *IEE Proc. Electr. Power Appl.*, **141**: 353–359, 1994.
43. N. Mutoh *et al.*, A motor driving controller suitable for elevators, *IEEE Trans. Power Electron.*, **13**: 1123–1134, 1998.
44. F. Abrahamsen, J. K. Pedersen, and F. Blaabjerg, State-of-art of optimal efficiency control of low cost induction motor drives, *Proc. Power Electronics and Motion Control Conf. PEMC'96*, part 2, Budapest, Hungary, 163–170, 1996.
45. I. Kioskeridis and N. Margaris, Loss minimization in scalar-controlled induction motor drives with search controllers, *IEEE Trans. Power Electron.*, **11**: 213–220, 1996.
46. G. C. D. Sousa, B. K. Bose, and J. G. Cleland, Fuzzy logic based on-line efficiency optimization control of an indirect vector-controlled induction motor drive, *IEEE Trans. Ind. Electron.*, **42**: 192–198, 1995.
47. B. K. Bose, N. R. Patel, and K. Rajashekara, A neuro-fuzzy-based on-line efficiency optimization control of a stator flux-oriented direct vector-controlled induction motor drive, *IEEE Trans. Ind. Electron.*, **44**: 270–273, 1997.
48. D. S. Kirschen, D. W. Novotny, and W. Suwanwisoot, Minimizing induction motor losses by excitation control in variable frequency drives, *IEEE Trans. Ind. Appl.*, **IA-20**: 1244–1250, 1984.
49. G. O. Garcia *et al.*, An efficient controller for an adjustable speed induction motor drive, *IEEE Trans. Ind. Electron.*, **41**: 533–539, 1994.
50. F. F. Bernal, A. G. Cerrada, and R. Faure, Model-based loss minimization for DC and AC vector-controlled motors including core saturation, *IEEE Trans. Ind. Appl.*, **36**: 755–763, 2000.
51. J. H. Chang and B. K. Kim, Minimum-time minimum-loss speed control of induction motors under field-oriented control, *IEEE Trans. Ind. Electron.*, **44**: 809–815, 1997.
52. I. Kioskeridis and N. Margaris, Loss minimization in induction motor adjustable-speed drives, *IEEE Trans. Ind. Electron.*, **43**: 226–231, 1996.
53. K. Matsuse *et al.*, High-response flux control of direct-field-oriented induction motor with high efficiency taking core loss into account, *IEEE Trans. Ind. Appl.*, **35**: 62–69, 1999.
54. S. N. Vukosavic and E. Levi, Robust DSP-based efficiency optimisation of a variable speed induction motor drive, *IEEE Trans. Ind. Electron.*, **50**: 560–570, 2003.
55. K. Rajashekara, A. Kawamura andK. Matsuse (eds.), *Sensorless Control of ac Motor Drives*, Piscataway, NJ: IEEE Press, 1996.
56. P. Vas, *Sensorless vector and direct control*, Oxford: Oxford University Press, 1998.
57. C. Schauder, Adaptive speed identification for vector control of induction motors without rotational transducers, *IEEE Trans. Ind. Appl.*, **28**: 1054–1061, 1992.
58. J. Hu and B. Wu, New integration algorithms for estimating motor flux over a wide speed range, *IEEE Trans. Power Electron.*, **13**: 969–977, 1998.
59. V. Vasic, S. N. Vukosavic, and E. Levi, A stator resistance estimation scheme for speed sensorless rotor flux oriented induction motor drives, *IEEE Trans. Energy Convers.*, **18**: 476–483, 2003.
60. E. Levi and M. Wang, A speed estimator for high performance sensorless control of induction motors in the field weakening region, *IEEE Trans. Power Electron.*, **17**: 365–378, 2002.
61. G. C. Verghese and S. R. Sanders, Observers for flux estimation in induction machines, *IEEE Trans. Ind. Electron.*, **35**: 85–94, 1988.
62. T. Du, P. Vas and F. Stronach, Design and application of extended observers for joint state and parameter estimation in high-performance ac drives, *IEE Proc. Electr. Power Appl.*, **142**: 71–78, 1995.
63. D. J. Atkinson, P. P. Acarnley and J. W. Finch, Observers for induction motor state and parameter estimation, *IEEE Trans. Ind. Appl.*, **27**: 1119–1127, 1991.
64. L. Salvatore, S. Stasi and L. Tarchioni, A new EKF-based algorithm for flux estimation in induction machines, *IEEE Trans. Ind. Electron.*, **40**: 496–504, 1993.

Reading List

M. P. Kazmierkowski and H. Tunia, *Automatic Control of Converter-fed Drives*, Amsterdam: Elsevier, 1994. (Good textbook with wide coverage of electric drive control; contains excellent reference section with literature published until 1990.)

S. A. Nasar and I. Boldea, *Electric Machines: Dynamics and Control*, Boca Raton, FL: CRC Press, 1993. (Somewhat similar in approach and content to Ref. 1, but less detailed).

B. K. Bose (ed.), *Power Electronics and Variable Frequency Drives*, Piscataway, NJ: IEEE Press, 1997. (A collection of exceptionally fine and in-depth articles, some of them at an advanced level.)

A. M. Trzynadlowski, *Control of induction motors*, San Diego: Academic Press, 2001. (An excellent textbook, devoted entirely to the variable speed induction motor drives; covers all relevant aspects and includes chapters on direct torque control and speed-sensorless control).

R. Krishnan, *Electric Motor Drives: Modelling, Analysis and Control*, Upper Saddle River: Prentice Hall, 2001. (Probably the most detailed treatment of variable speed AC drives currently available in a single textbook. Includes detailed coverage of parameter variation effects and compensation schemes for vector controlled induction motor drives. Of special value is a section on the design of the speed controller, a topic that is rarely covered in drives textbooks).

B. K. Bose, *Modern Power Electronics and AC Drives*, Upper Saddle River: Prentice Hall, 2002. (Broad coverage of both power electronic converters and variable speed drives; includes both induction and synchronous motor drives, as well as details of the artificial intelligence techniques as applied in AC motor drives).

References 5, 7, 9, 11, 30 and 40 contain exhaustive bibliographies. Reference 55 contains an exceptional collection of most important early papers in the area of speed-sensorless vector control.

EMIL LEVI
Liverpool John Moores
University
Liverpool, United Kingdom